20. STABLE ISOTOPE AND TRACE ELEMENT GEOCHEMISTRY OF CARBONATE SEDIMENTS ACROSS THE CRETACEOUS/TERTIARY BOUNDARY AT DEEP SEA DRILLING PROJECT HOLE 577, LEG 86[1]

James C. Zachos and Michael A. Arthur, University of Rhode Island
Robert C. Thunell, Douglas F. Williams, and Eric J. Tappa, University of South Carolina[2]

ABSTRACT

Detailed analyses of well-preserved carbonate samples from across the Cretaceous/Tertiary boundary in Hole 577 have revealed a significant decline in the $\delta^{13}C$ values of calcareous nannoplankton from the Maestrichtian to the Danian Age accompanied by a substantial reduction in carbonate accumulation rates. Benthic foraminifers, however, do not exhibit a shift in carbon composition similar to that recorded by the calcareous nannoplankton, but actually increase slightly over the same time interval. These results are similar to the earlier findings at two North Pacific Deep Sea Drilling Project locations, Sites 47.2 and 465, and are considered to represent a dramatic decrease in oceanic phytoplankton production associated with the catastrophic Cretaceous/Tertiary boundary extinctions. In addition, the change in carbon composition of calcareous nannoplankton across the Cretaceous/Tertiary boundary at Hole 577 is accompanied by only minor changes in the oxygen isotope trends of both calcareous nannoplankton and benthic foraminifers, suggesting that temperature variations in the North Pacific from the late Maestrichtian to the early Danian Age were insignificant.

INTRODUCTION

The uncertain origin of the biotic extinctions at the Cretaceous/Tertiary boundary is one of the more intriguing problems in paleoceanography. A plethora of models have been proposed to account for the pattern and timing of the extinctions (e.g., Silver and Schultz, 1982), but many of the published papers are based on relatively few data. A recently popular explanation is that of an extraterrestrial cause for the extinctions. An early paper by Alvarez et al. (1980) reported the discovery of anomalous concentrations of iridium and other platinum group metals (siderophile elements) in a clay layer at the Cretaceous/Tertiary boundary at Gubbio, Italy. Since that time, they and a number of other workers have recorded similar enriched zones at the boundary in at least 19 other globally distributed sites, including several terrestrial (nonmarine) sequences (Alvarez et al., 1982). It appears that, on the basis of the distribution of the Ir anomalies and the ratios of platinum group metals to one another, there was an impact of an extraterrestrial object with the earth at the end of the Maestrichtian Age. However, the significance of the iridium anomaly as evidence of an impact signature has been questioned (e.g., Officer and Drake, 1983; McLean, 1982). Abrupt extinctions of many taxa of Cretaceous marine plankton occur in conjunction with the Ir anomaly, but the relationship that the major impact (or other) event had to the biotic extinctions is not yet clear.

Alvarez et al. (1980, 1982) proposed a "lights out" scenario, whereby the dust or ejecta thrown up into the atmosphere by the impact would lead to a period of darkness lasting several years. This episode of darkness is proposed to have led to cessation of photosynthesis, extinction of most phytoplankton, and resulting effects on down the marine and terrestrial food chains. More recent modeling suggests that the period of darkness would have been much shorter, on the order of 3 to 6 months (Toon et al., 1982; Thierstein, 1982). Other authors have proposed variants of the impact hypothesis, including extinction by chemical poisoning related to the impact of a cometary body (Hsü, 1980), catastrophic warming related to drastic increases in atmospheric water vapor as the result of an ocean impact and resulting thermal stress on organisms (Emiliani et al., 1981), and sudden cooling as the result of global albedo increases from high concentrations of atmospheric dust (Toon et al., 1982). These hypotheses are not mutually exclusive and the suggested mechanisms could have, in combination, affected the terrestrial and marine biotas.

Other workers (e.g., Bramlette, 1965; Tappan, 1968; Fischer and Arthur, 1977; Vogt, 1972; McLean, 1980, 1982) have provided models for the biotic extinctions at the Cretaceous/Tertiary boundary that require causes internal to the earth. Vogt (1972), McLean (1980, 1982), and Zoller et al. (1983) suggested increased rates of volcanism at the end of the Cretaceous. The biotic extinctions would therefore be related to either trace metal poisoning, increased atmospheric pCO_2 and sudden global climatic warming, and/or decreased oceanic surface water pH. Others (Bramlette 1965; Tappan, 1968; Fischer and Arthur, 1977) suggested that increased extinction rates at the end of the Cretaceous were the result of marine regression, oceanic nutrient deficiencies, and global cooling. Needless to say, the variety of mechanisms proposed and the often contradictory hypotheses (e.g., warming vs. cooling) point to the need for much more data bearing on rates of extinction, environmental tolerances, and paleoclimate and paleoproductivity estimates. Thus, high resolution studies of complete marine Cretaceous/Tertiary boundary sequences are needed.

[1] Heath, G. R., Burckle, L. H., et al., *Init. Repts. DSDP*, 86: Washington (U.S. Govt. Printing Office).

[2] Addresses: (Zachos, Arthur) Graduate School of Oceanography, University of Rhode Island, Kingston, RI 02882; (Thunell, Williams, Tappa) Department of Geology, University of South Carolina, Columbia, SC 29208.

We have examined geochemical and stable isotopic compositions of sediment and calcareous microfossils in pelagic–hemipelagic sequences across the Cretaceous/Tertiary boundary at a number of sites in the Pacific, the North Atlantic, and the South Atlantic Ocean basins (Zachos et al., unpubl. data; Williams et al., 1983). Our intent is to provide high resolution chemical and stable-isotopic profiles across the Cretaceous/Tertiary boundary in order to evaluate possible changes in carbonate preservation, which might affect the stable-isotope signals from calcareous plankton, and to evaluate climatic, paleoceanographic or oceanic chemical changes that may have occurred at the boundary.

In this chapter we present stable isotopic and geochemical data from Cretaceous/Tertiary boundary sequences recovered at two Deep Sea Drilling Project (DSDP) sites in the Pacific, Sites 47.2 and 577 (Fig. 1). The Site 47.2 sequence is apparently disturbed by drilling. Site 577, which was hydraulically piston cored during Leg 86 (Site 577 chapter, this volume), offers an undisturbed Cretaceous/Tertiary boundary transition in a pelagic carbonate facies deposited at relatively high sedimentation rates. Preservation of calcareous microfossils is good as we show in scanning electron micrographs and trace element geochemical data (Sr/Ca, Mn) presented in this chapter. We compare our stable-isotope results with those from Boersma and Shackleton (1981) from Pacific Site 465 (Figs. 4 and 5). We also discuss the implications of stable-isotopic data from carbonate fine-fraction, planktonic and benthic foraminifers and changes in carbonate accumulation rates across the boundary for paleoceanographic events at the end of the Cretaceous through the early Paleocene.

ANALYTICAL METHODS

Bulk samples were weighed, disaggregated, and wet sieved through a 63-μm screen. The less than 63-μm fraction was then thoroughly washed with deionized water through 0.45-μm metricel filters in a vacuum apparatus. The washed specimens were then prepared for stable-

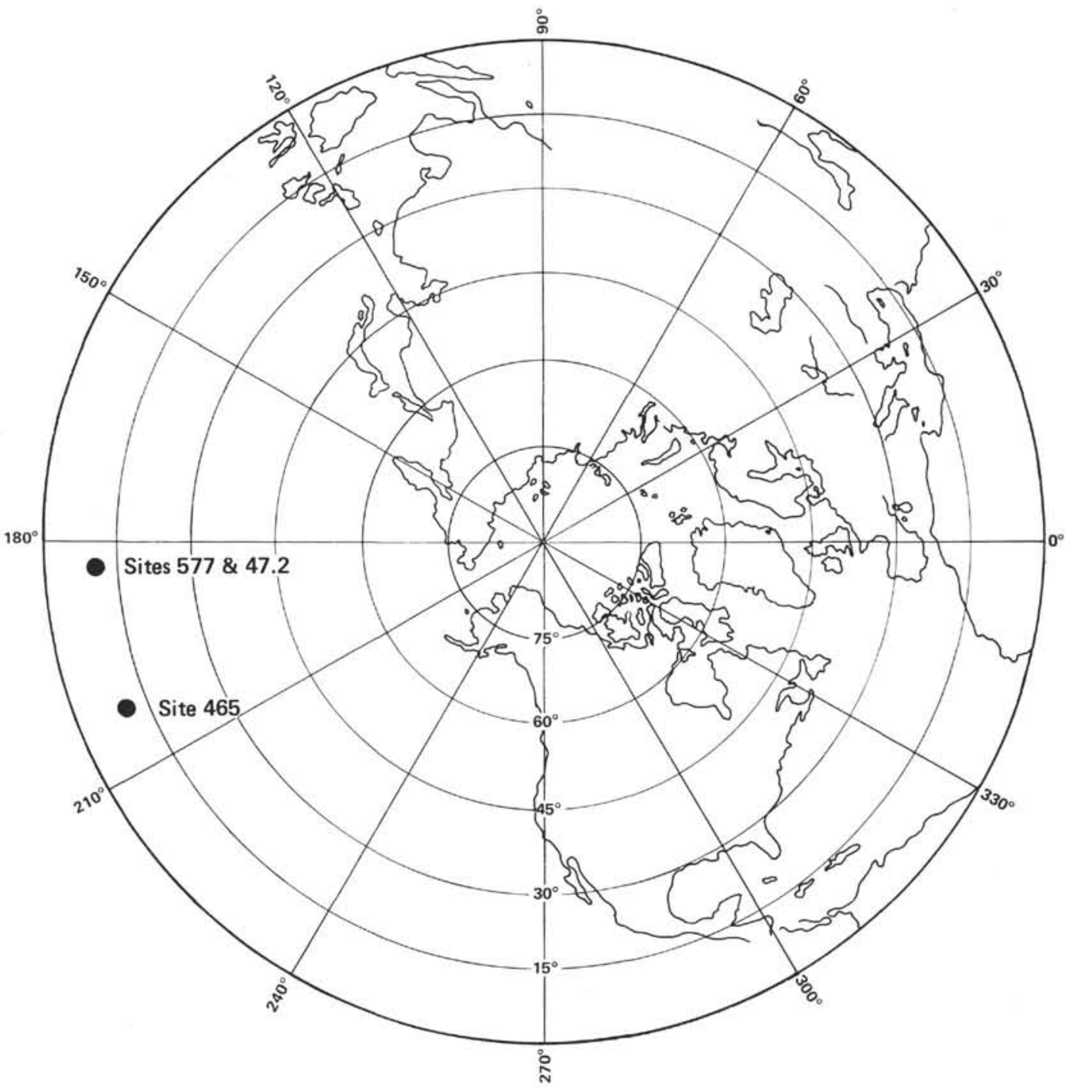

Figure 1. The paleopositions of Sites 577, 465, and 47.2 in the Northern Hemisphere 70 m.y. ago (after Firstbrook et al., 1979; Lancelot and Larson, 1975). Sites 577 and 47.2 are located on the Shatsky Rise. Site 465 is located on the nearby Hess Rise.

isotope analysis in the following manner. The samples were first roasted at 400°C under vacuum for 1 hr. and then reacted in 100% orthophosphoric acid at 50°C. Isotopic analyses were preformed on a VG Micromass 602D isotope ratio mass spectrometer. All samples were measured relative to a laboratory standard reference gas and are reported in notation as per mil deviations from PDB.

$$\delta(‰) = \left(\frac{\text{R sample}}{\text{R standard}} - 1\right) \times 10^3$$

Calibration of the reference gas was achieved by analysis of B-1 standard, which has a measured value of +0.06‰ for $\delta^{18}O$ and +0.64‰ for $\delta^{13}C$ relative to PDB (Keigwin, 1980). Precision of isotopic analyses is better than +0.11 per mil for oxygen and +0.08 per mil for carbon.

Trace-element measurements were conducted on the less than 63 μm carbonate fraction. Each sample was thoroughly washed with deionized water to remove sea salts, dried, and finely ground. The samples (0.1 g) were then dissolved in 0.7 *N* acetic acid to avoid stripping of ions from clay minerals as much as possible, filtered, and diluted to 100 ml. Magnesium, strontium, and manganese concentrations were then determined with a Perkins Elmer Model 503 Atomic Absorbtion Spectrophotometer. All results are reported in ppm. Analytical precision for Mg is ±5%, for Mn ±3%, and for Sr ±8%. Although we also analyzed the same samples for Ca, the analytical precision was much lower (±20%) than for the other elements. We have used calculated Ca values from carbonate contents, assuming pure $CaCO_3$. This technique has worked well for other Cretaceous pelagic carbonate sequences where analytical Ca and total $CaCO_3$ contents were obtained (Dean and Arthur, unpubl. data) and introduces less variation due to poor precision than the atomic absorption method. Percent calcium carbonate was determined by the bomb method (Müller and Gastner, 1971).

Carbonate accumulation rates (CAR) (Table 4) were determined using the following equation:

$$\text{CAR} = (\%CaCO_3/100)\{[(W\ \text{g/cm}^3) - (P/100)(1.01\ \text{g/cm}^3)](S\ \text{cm/yr.})\}$$

where *P* is porosity and *W* is wet bulk density. Sedimentation rates (*S*) were determined from magneto- and biostratigraphies.

STABLE-ISOTOPE RESULTS

Planktonic Calcareous Microfossils

Results of oxygen- and carbon-isotope analyses of Maestrichtian and Danian fine fraction (<63 μm) $CaCO_3$ and benthic foraminifers from Hole 577[3] and whole rock $CaCO_3$ from Site 47.2 are given in Tables 1 and 2 and shown in Figures 2 and 3. Carbon- and oxygen-isotope analyses were performed on samples of carbonate fine fraction from the top of Section 577-12-2 (*Chiasmolithus danicus*, nannofossil Zone CP2, 101–106 m sub-bottom depth) to the bottom of Section 577-13-4 (*Micula murus* nannofossil Zone, 109–117.6 m sub-bottom depth) at Hole 577 and from the top of Section 47.2-10-6 (*Cruciplacolithus tenuis*, CP1b Subzone) to the bottom of Section 47.2-12-2 (*M. murus* Zone) at Site 47.2. Sample spacing ranged from 10- to 20-cm intervals although the spacing interval was reduced to 5 cm near the Cretaceous/Tertiary boundary at each site.

Oxygen-isotope values of Hole 577 carbonate fine-fraction samples from the *M. murus* zone varied only slightly upcore, averaging −1.0 ± 0.05‰ throughout (Fig. 2). Values begin to increase slightly near the top of this zone several centimeters below the Cretaceous/Tertiary boundary, reaching a peak of −0.49‰ at Sample 577-12-5, 99 cm. Above this level, through the *Markalius inversus* and *C. tenuis* zones (106 to 109 m sub-bottom depth), $\delta^{18}O$ values vary considerably, fluctuating between a low of −1.45‰ in Sample 577-12-3, 110 cm and high value of −0.16‰ in Sample 577-12-4, 110 cm.

Site 47.2 Maestrichtian $\delta^{18}O$ values are only an average of 0.1‰ heavier than the $\delta^{18}O$ values of corresponding samples from Hole 577 (Figs. 3 and 4). Similarly, the Danian oxygen-isotope ratios are also just slightly heavier than the corresponding values from Hole 577.

$\delta^{13}C$ values of carbonate fine-fraction samples from the *M. murus* Zone are relatively constant, averaging 2.65 ± 0.2‰ (Fig. 2). At the Cretaceous/Tertiary boundary, there is a sharp decrease of 1.0‰ over a 10-cm interval which coincides with a layer of slightly lower than average carbonate content. Further upcore, through the *C. tenuis* nannofossil Zone, $\delta^{13}C$ values remain relatively low between 1.7 and 2.3‰. A similar shift in $\delta^{13}C$ is recorded in the Site 47.2 bulk $CaCO_3$ samples (Fig. 3). Maestrichtian samples at Site 47.2 yield average $\delta^{13}C$ values of 2.6 ±0.2‰ compared to values of 1.75 ± 0.1‰ for Danian samples, with the actual carbon-isotope shift occurring somewhere between Samples 47.2-11-5, 25 cm and 47.2-11-3, 100 cm. The major shift apparently coincides with the Cretaceous/Tertiary boundary determined from calcareous nannofossils (Thierstein, 1981). Anomalous points in both the Maestrichtian and Danian sections are probably an artifact of displaced or mixed sediments resulting from coring disturbances.

Stable carbon-isotope compositions of planktonic foraminifers from Site 465 (Boersma and Shackleton, 1981) on the Hess Rise have been plotted against an absolute time framework in Figure 5 along with the data from Sites 577 and 47.2 for comparison using the chronology shown in Figure 6. Boersma and Shackleton (1981) determined Maestrichtian and Danian near-surface-water carbon-isotope values at Site 465 by analyzing *Rugoglobigerina* and *Guembelitria*, respectively. The absolute shift in $\delta^{13}C$ (surface water) at Site 465 as recorded in the tests of these planktonic foraminifers is greater (2.2‰) than the shifts found at Sites 577 and 47.2 as measured in the fine fraction $CaCO_3$ (Fig. 5). However, because the carbon-isotope anomalies at Hole 465 were not determined on a single species across the boundary, this rather large shift may be partially a function of differences in species vital effects, although it is unlikely that the entire shift could be attributed to this. A further possibility is that the measured values reflect actual differences in the carbon composition of surface waters overlying these two locations; however, given the relative proximity of the Shatsky and Hess rises and their central paleoposition in the Pacific, this also seems unlikely.

Benthic Foraminiferal Isotope Records

Since many species of benthic foraminifers survived the Cretaceous/Tertiary boundary extinctions (Douglas and Woodruff, 1981), one may assume that it would be

[3] Subsequent to completion of this manuscript a recalibration of standard values was conducted at the Graduate School of Oceanography stable-isotope lab which affects the conversion of measured values to PDB. As a result, Hole 577 oxygen and carbon stable-isotope values reported here in tables, text, and illustrations should be corrected by adding 0.42‰ and 0.13‰ respectively. The change in oxygen-isotope values amounts to less than 2°C in paleotemperature estimates.

Table 1. Stable-isotope results from Hole 577.

Core-Section (interval in cm)	Depth (m)	% $CaCO_3$	% >63 μm	Sample type	$\delta^{18}O_{PDB}$	$\delta^{13}C_{PDB}$
12-2, 49-51	103.8	93	7	Fine fraction	−1.30	2.03
12-2, 69-71	104	91.9	1	Fine fraction	−1.42	1.95
12-2, 89-91	104.2	91.6	1	Fine fraction	−1.37	2.13
12-2 99-101	104.3	92.8	3	Fine fraction	−0.90	2.09
12-2, 129-131	104.6	94.5	3	Fine fraction	−1.27	2.02
12-3, 9-11	104.9	89.7	3	Fine fraction	−1.24	1.89
12-3, 29-31	105.1	93.9	1	Fine fraction	−0.97	2.04
12-3, 49-51	105.3	91.3	1	Fine fraction	−1.08	2.18
12-3, 69-71	105.5	92.5	1	Fine fraction	−0.95	2.27
12-3, 89-91	105.7	87.9	1	Fine fraction	−1.37	2.06
12-3, 109-111	105.9	94.85	3	Fine fraction	−1.45	1.92
12-3, 129-131	106.1	92.7	11	Fine fraction	−1.30	2.04
12-4, 9-11	106.4	95.4	14	Fine fraction	−1.09	2.00
12-4, 29-31	106.6	95.6	18	Fine fraction	−1.13	1.98
12-4, 49-51	106.8	93.1	20	Fine fraction	−1.24	1.73
12-4, 69-71	107	95.6	27	Fine fraction	−0.85	1.75
12-4, 89-91	107.2	94.5	25	Fine fraction	−0.34	1.87
12-4, 109-111	107.4	95.2	23	Fine fraction	−0.16	1.85
12-5, 19-21	108	93.1	20	Fine fraction	−0.85	1.78
12-5, 39-41	108.2	91.3	28	Fine fraction	−0.95	1.83
12-5, 59-61	108.4	93.1	25	Fine fraction	−0.90	1.84
12-5, 79-81	108.6	93.7	24	Fine fraction	−0.87	1.98
12-5, 91-93	108.72	93	14	Fine fraction	−0.70	2.19
12-5, 98-100	108.89	91.5	16	Fine fraction	−0.49	2.15
12-5, 108-109	108.99	93.2	15	Fine fraction	−0.83	2.02
12-5, 113-114	109.44	93.5	13	Fine fraction	−0.63	2.02
12-5, 117-119	109.09	89.5	9	Fine fraction	−0.65	1.91
12-5, 125-126	109.16	88.2	6	Fine fraction	−0.73	2.03
12-5, 128-130	109.19	88.8	3	Fine fraction	−0.74	2.49
12-5, 131-132	109.22	94.8	1	Fine fraction	−0.82	2.83
12-5, 134-136	109.26	95.7	<1	Fine fraction	−0.64	2.94
12-5, 144-145	109.35	96	<1	Fine fraction	−0.97	2.87
12-6, 19-21	109.6	95.2	<1	Fine fraction	−0.81	2.76
12-6, 39-41	109.8	96.1	<1	Fine fraction	−0.85	2.55
12-6, 59-61	110	94.8	<1	Fine fraction	−0.87	2.55
12-6, 99-101	110.4	95.2	<1	Fine fraction	−0.93	2.50
12-7, 9-11	111	93.6	<1	Fine fraction	−0.94	2.64
13-1, 59-61	111.8	87.4	<1	Fine fraction	−1.08	2.48
13-1, 99-101	112.2	94	<1	Fine fraction	−1.05	2.49
13-1, 139-141	112.6	95.38	<1	Fine fraction	−0.99	2.83
13-2, 39-41	113.1	96.3	<1	Fine fraction	−1.10	2.80
13-2, 79-81	113.5	94.5	<1	Fine fraction	−1.03	2.78
13-2, 119-121	113.9	94.8	<1	Fine fraction	−1.05	2.76
13-3, 19-21	114.4	94	<1	Fine fraction	−0.97	2.72
13-3, 59-61	114.8	94.6	<1	Fine fraction	−0.94	2.80
13-3, 99-101	115.2	90.9	<1	Fine fraction	−0.95	2.65
13-3, 139-141	115.6	95.1	<1	Fine fraction	−0.93	2.86
13-4, 39-41	116.1	94.1	<1	Fine fraction	−0.99	2.71
13-4, 99-101	116.7	94.9	<1	Fine fraction	−0.87	2.64
12-2, 89-91				*Aragonia*	−0.05	0.81
12-2, 129-131				*Aragonia*	0.08	0.88
12-3, 9-11				*Aragonia*	−0.08	0.60
12-4, 89-91				*Aragonia*	0.05	1.21
12-5, 59-61				*Aragonia*	0.48	1.98
12-5, 79-81				*Aragonia*	0.39	1.90
12-5, 117-119				*Aragonia*	0.20	1.65
12-5, 125-126				*Aragonia*	0.15	1.61
12-5, 108-109				*Aragonia*	0.45	1.82
12-5, 128-130				*Aragonia*	0.04	1.65
12-6, 19-21				*Aragonia*	0.31	1.36
12-6, 59-61				*Aragonia*	−0.33	0.82

fairly easy to reconstruct monospecific benthic stable-isotope records across the boundary. However, species of benthic foraminifers that are abundant in Danian samples are often present but not abundant in Maestrichtian samples and vice versa. In addition, the dilution of coarse-fraction foraminifers by calcareous nannofossils (predominance of fine fraction) in Maestrichtian sediments makes it extremely difficult to find the necessary number of a specific benthic foraminifer from the small sample sizes available at the closely spaced intervals needed to conduct stable-isotope analyses. In this case, analyses of mixed benthic assemblages, which provide less reliable data, must be performed instead. At Hole 577 we were fortunate enough to find one genus of benthic foraminifer, *Aragonia* (Plate 2, Figs. 1, 3, and 4), that was both relatively plentiful and present in a few samples from either side of the boundary. The measured $\delta^{13}C$ values of late Maestrichtian *Aragonia* indicate a carbon-isotope trend toward heavier values just below the boundary, increasing from +0.83‰ a meter below the boundary (Sample 577-12-6, 79 cm) to +1.38‰ at the boundary (Sample 577-12-5, 125 cm). This trend continues in

Table 2. Stable-isotope results from Site 47.2.

Core-Section (interval in cm)	% >63 μm	Sample type	$\delta^{18}O_{PDB}$	$\delta^{13}C_{PDB}$
10-6, 50-51	4	Whole rock	−0.97	2.05
10-6, 100-101	8	Whole rock	−1.13	2.04
10-6, 127-128	4	Whole rock	−1.31	1.99
11-1, 25-26	16	Whole rock	−1.15	1.38
11-1, 75-77	19	Whole rock	−0.86	1.39
11-1, 125-126	20	Whole rock	−0.98	1.62
11-2, 30-31	18	Whole rock	−0.72	1.66
11-2, 50-51	20	Whole rock	−0.76	1.71
11-2, 100-101	18	Whole rock	−0.61	1.93
11-3, 30-31	1	Whole rock	−0.74	2.80
11-3, 60-61	7	Whole rock	−0.74	2.19
11-3, 100-101	15	Whole rock	−0.76	1.96
11-3, 125-126	16	Whole rock	−0.70	1.90
11-3, 138-139	14	Whole rock	−0.67	1.90
11-4, 30-31	1	Whole rock	−0.97	2.66
11-4, 60-61	4	Whole rock	−0.92	2.66
11-4, 80-81	3	Whole rock	−0.88	2.64
11-4, 98-99	10	Whole rock	−0.83	2.10
11-4, 120-121	4	Whole rock	−0.85	2.14
11-4, 138-139	9	Whole rock	−0.91	2.28
11-5, 10-11	5	Whole rock	−0.94	2.48
11-5, 20-21	5	Whole rock	−0.91	2.52
11-5, 27-28	<1	Whole rock	−0.90	2.43
11-5, 30-31	<1	Whole rock	−0.90	2.76
11-5, 48-49	<1	Whole rock	−1.01	2.42
11-5, 70-71	<1	Whole rock	−0.78	2.69
11-5, 90-91	<1	Whole rock	−0.85	2.73
11-5, 110-111	<1	Whole rock	−0.87	2.75
11-5, 127-128	<1	Whole rock	−0.92	2.65
11-5, 140-141	<1	Whole rock	−0.77	2.65
11-6, 23-24	<1	Whole rock	−0.89	2.58
11-6, 40-41	<1	Whole rock	−0.78	2.57
11-6, 60-61	<1	Whole rock	−0.84	2.74
11-6, 80-81	<1	Whole rock	−0.70	2.72
11-6, 125-126	<1	Whole rock	−0.89	2.74
12-1, 25-26	<1	Whole rock	−0.92	2.52
12-1, 75-76	<1	Whole rock	−1.10	2.39
12-1, 125-126	<1	Whole rock	−0.98	2.79
12-2, 25-26	<1	Whole rock	−0.93	2.81
12-2, 68-69	<1	Whole rock	−1.01	2.73
12-2, 100-101	<1	Whole rock	−1.02	2.75
12-2, 125-127	<1	Whole rock	−1.07	2.75

the Danian section, reaching a maximum value of 1.98‰ in Sample 577-12-5, 60 cm. Further upcore, in Sections 577-12-2 and 577-12-3, *Aragonia* values return to preboundary levels, decreasing by as much as 1.2‰.

A similar trend across the Cretaceous/Tertiary boundary, but of lesser magnitude, is exhibited in the Site 465 carbon-isotope values of another benthic foraminifer, *Bulimina* (Fig. 4; Boersma and Shackleton, 1981). The $\delta^{13}C$ values of Maestrichtian *Bulimina* become enriched by 0.5‰, relative to earlier late Maestrichtian values, prior to the boundary. Above this point, the carbon isotopic composition of *Bulimina* decreases by about 0.4‰ up to 65.5 m.y. ago (above the Cretaceous/Tertiary boundary). There appears to be a slight discrepancy between the two benthic isotope records in both the overall trend and time of change, although the overall magnitude of the isotope values are similar. Because the analyses of benthic foraminifers at these two sites were performed on different species, *Bulimina* and *Aragonia*, the discrepancies between the two isotope records may be attributable to differences in species vital effects. In fact, different species of modern benthic foraminifers from the same samples have been found to possess significantly different $\delta^{13}C$ values and may also show considerable intraspecific variation between various size fractions (Woodruff et al., 1980; Belanger et al., 1981; Savin and Yeh, 1981).

Oxygen-isotope analyses of *Aragonia* in Hole 577 show no prominent trends (range ~0.5‰) although additional analyses of Core 13 samples should be conducted in order to determine whether the anomalous Maestrichtian value (Sample 577-12-6, 70 cm) is significant (Fig. 2). Overall, the $\delta^{18}O$ values are 0.8–1.5‰ heavier than the values obtained for planktonic organisms and roughly equivalent to the values obtained for Site 465 *Bulimina* (Fig. 4).

TRACE-ELEMENT GEOCHEMISTRY

Mineralogic stabilization of carbonate sediment occurs through solution–recrystallization processes. These processes also result in carbon- and oxygen-isotope stabilization. The stable-isotope values of altered carbonate sediments, therefore, may not represent the isotopic composition of the originally precipitated calcite, but rather some average of the isotopic composition of the original calcite and the reprecipitated calcite cements and overgrowths. In order to determine the extent of recrystallization, early investigators generally examined the downhole changes of various textural parameters such as porosity and cementation. However, more recently, chemical criteria have been considered in conjunction with textural studies, providing investigators with a quantitative as well as a qualitative measure of diagenesis (e.g., Matter et al., 1975). The distribution and concentration of certain trace elements such as strontium, magnesium, and manganese are known to change with increasing grades of diagenesis (e.g., Veizer, 1978; Baker et al., 1982). The direction of change is generally dependent upon the distribution coefficient of the element in question. Although contamination by noncarbonate fractions may prevent precise measurement of some elements such as Mn, the overall downhole trends and their signs provide us with important information for evaluating oxygen-isotope data that may have been influenced by diagenesis. The concentrations of the trace elements strontium, magnesium, and manganese in fine-fraction carbonates from across the Cretaceous/Tertiary boundary at Hole 577 are therefore reported and evaluated here (Table 3, Fig. 7).

The average measured value of magnesium for Site 577 samples falls within the typical range of values expected for a nannofossil ooze (Bathurst, 1981). From 116 to 109 m (the Cretaceous/Tertiary boundary) sub-bottom depth Mg concentrations range from 800 to 1300 ppm, varying very little throughout. From 109 to 108 m sub-bottom depth Mg concentrations increase sharply, reaching a peak value of 2100 ppm in Sample 577-12-5, 20 cm. This increase in Mg concentration coincides with an increase in fine-fraction insoluble residue contents (Fig. 7) over the same interval, suggesting that some Mg ions were leached from the clays during sample preparation. Above the Cretaceous/Tertiary bound-

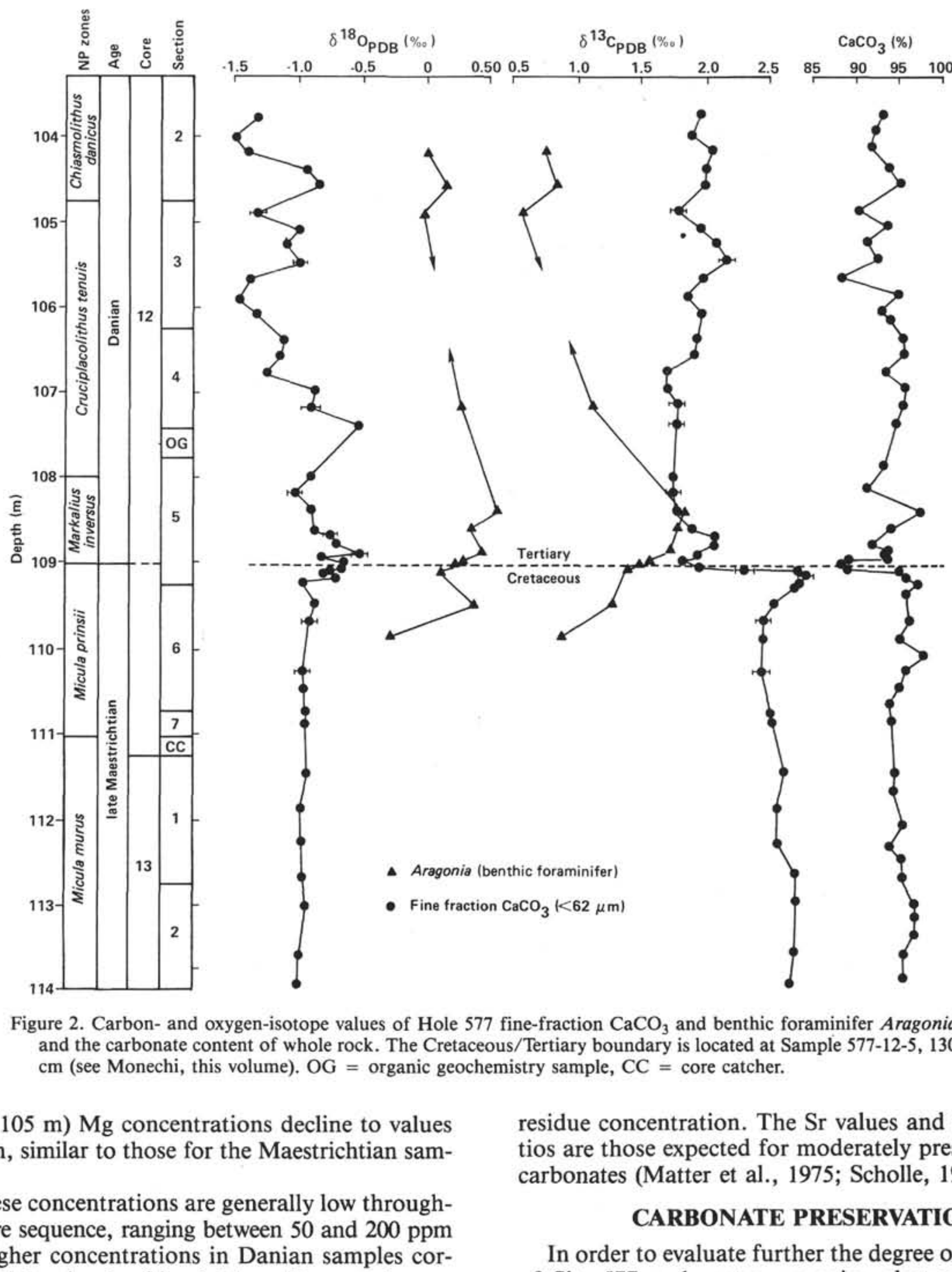

Figure 2. Carbon- and oxygen-isotope values of Hole 577 fine-fraction $CaCO_3$ and benthic foraminifer *Aragonia* and the carbonate content of whole rock. The Cretaceous/Tertiary boundary is located at Sample 577-12-5, 130 cm (see Monechi, this volume). OG = organic geochemistry sample, CC = core catcher.

ary (108 to 105 m) Mg concentrations decline to values of 1100 ppm, similar to those for the Maestrichtian samples.

Manganese concentrations are generally low throughout the entire sequence, ranging between 50 and 200 ppm (Fig. 7). Higher concentrations in Danian samples correspond to higher levels of insoluble residue, again suggesting that the measured concentrations of Mn were probably inflated by additional leached ions from manganese micronodules or other particles associated with the insoluble residue fraction.

Strontium content (and Sr/Ca ratio) varies very little in samples from below the boundary, ranging from 950 (Sample 577-12-6, 100 cm) to 1230 ppm (Sample 577-13-4, 100 cm) (Fig. 7). A sharp increase in Sr occurs just above the boundary between Samples 577-12-5, 109 cm and 577-12-5, 92 cm, with concentrations reaching 1700 ppm. Sr content declines rapidly upcore and, unlike Mg or Mn, exhibits no correspondence with the insoluble residue concentration. The Sr values and the Sr/Ca ratios are those expected for moderately preserved pelagic carbonates (Matter et al., 1975; Scholle, 1977).

CARBONATE PRESERVATION

In order to evaluate further the degree of preservation of Site 577 carbonates, scanning electron microscope (SEM) photographs were taken of foraminifer and coccolith tests and ultrastructure in conjunction with trace-element studies.

Adelseck et al. (1973) have demonstrated in laboratory experiments that calcite overgrowths and dissolution etching occur with greater frequency with increasing burial conditions (i.e., increased temperature and pressure). The dissolution and recrystallization of calcite in a calcareous ooze is such that cement overgrowths on the low magnesium calcite of large coccoliths and discoasters occur at the expense of planktonic foraminifers and small coccoliths, which usually disaggregate with

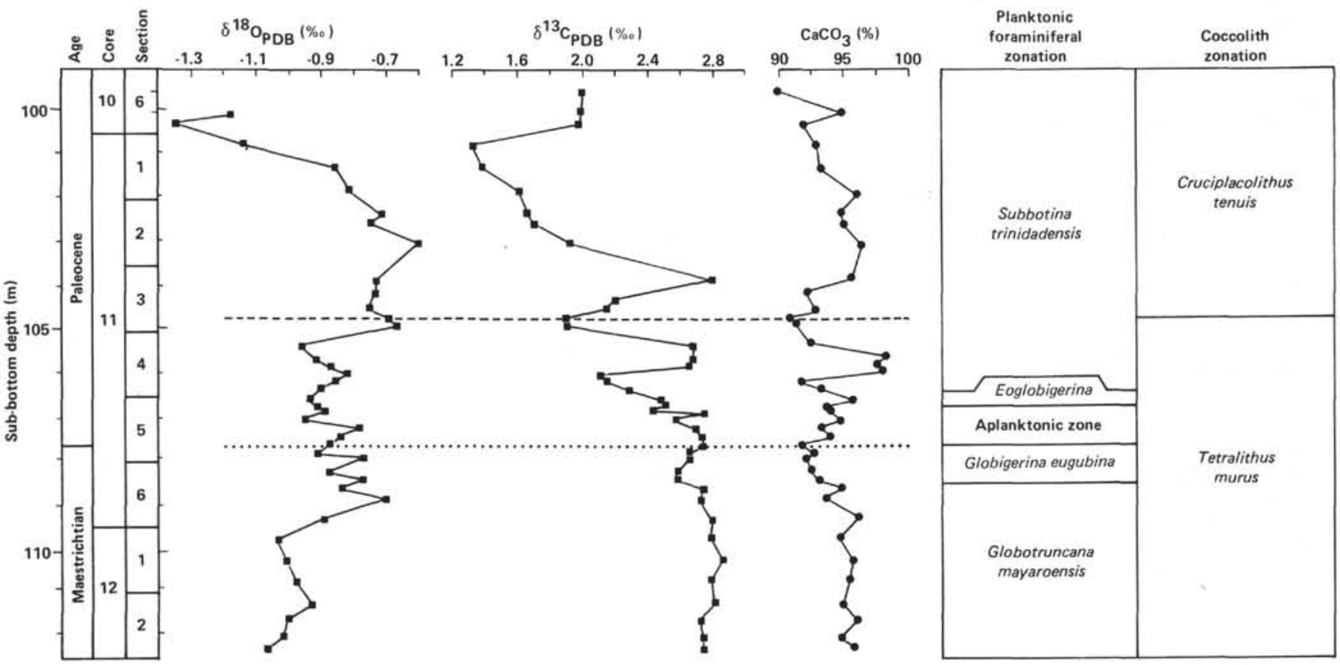

Figure 3. Site 47.2 carbon- and oxygen-isotope values and carbonate content of whole rock samples. Included are Cretaceous/Tertiary boundary locations based on planktonic foraminifer (dots; Hofker, 1978) and coccolith (dashed; Thierstein, 1981) biostratigraphy.

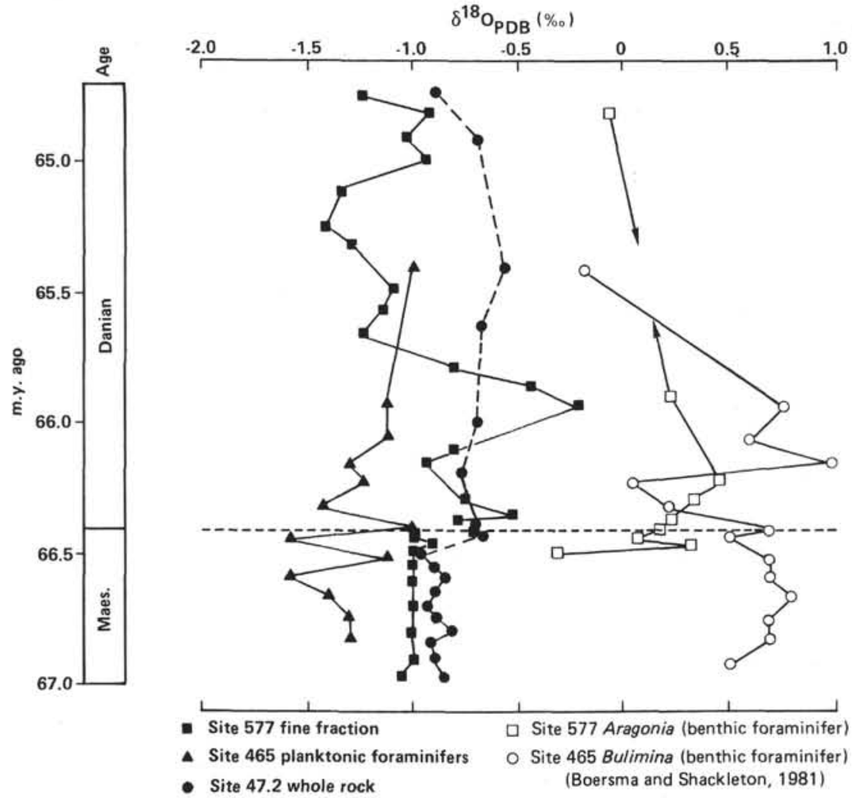

Figure 4. Cretaceous/Tertiary planktonic and benthic oxygen-isotope records from three North Pacific DSDP sites: 465 (data from Boersma and Shackleton, 1981), 47.2, and 577. Site 465 is located on the Hess Rise and 47.2 and 577 on the Shatsky Rise (see Fig. 1).

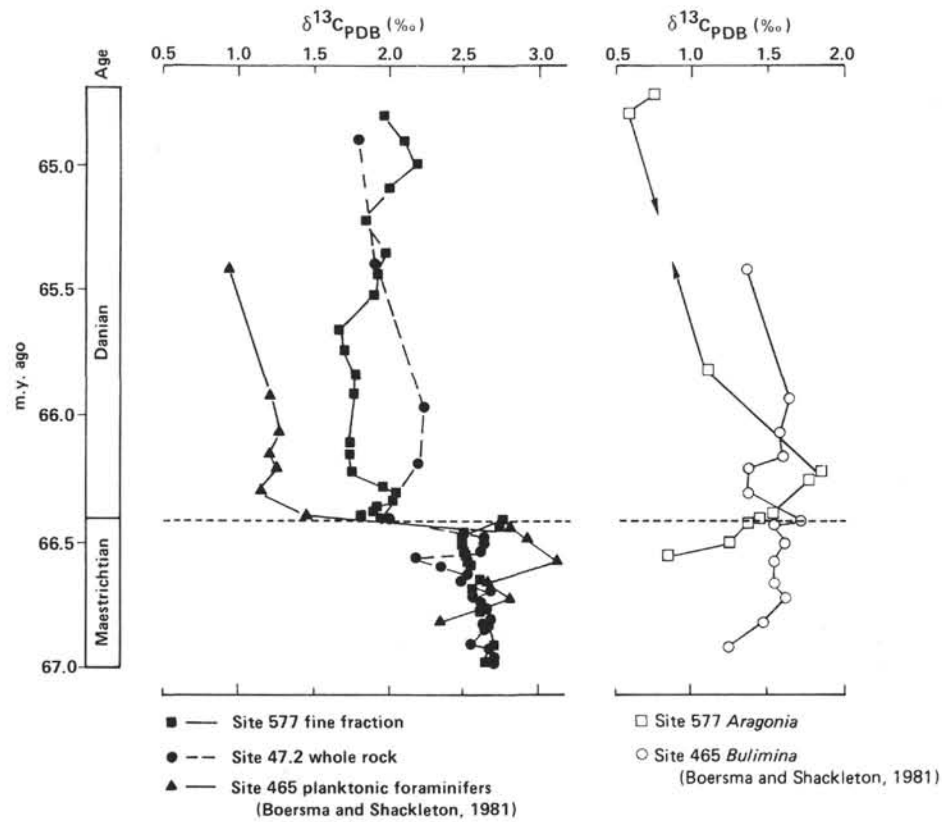

Figure 5. Compilation of planktonic and benthic carbon-isotope records from Sites 465 (data from Boersma and Shackleton, 1981), 47.2, and 577.

increasing dissolution (e.g., Douglas and Savin, 1971; Schlanger and Douglas, 1974; Roth and Berger, 1975; Berger, 1975; Thierstein, 1980; Thunell, 1982). As diagenesis progresses, cementation of grains generally follows, resulting in a transition from ooze to chalk to limestone. A well-preserved calcareous fossil assemblage should, therefore, exhibit the following physical characteristics: (1) individual specimens of foraminifers and nannofossils are essentially unbroken and free of extensive etchings or overgrowths, and (2) cementation between grains is absent. If signs of extensive diagenetic alteration do exist, then stable-isotope values must be considered suspect.

SEM photographs of Site 577 Danian and Maestrichtian samples show moderately to well-preserved calcareous microfossil specimens. Coccoliths from Maestrichtian samples in Hole 577 (Plate 4, Figs. 5–8) exhibit some signs of incipient dissolution and recrystallization.

Overall, the preservation of Maestrichtian calcareous nannofossils is moderate at Site 577. Euhedral calcite overgrowths are present on some coccoliths and some specimens are etched or partially dissolved and disaggregated (Plate 4, Figs. 7 and 8). Similar structures have been found on coccoliths from Site 47.2 (Plate 1, Fig. 3 and 4). Earlier calcareous nannofloral work at Site 47.2 (Thierstein, 1981) revealed a large increase in the proportions of dissolution-resistant taxa, such as *Micula staurophora* and *M. murus* in the middle sections of Core 11, suggesting either slight pre- or postburial dissolution. However, because the sediments at Site 47.2 have been mechanically displaced and mixed, it is difficult to determine exactly where stratigraphically, relative to the Cretaceous/Tertiary boundary, the dissolution may have occurred.

Danian samples from both Sites 577 and 47.2 (Plate 1, Fig. 2; Plate 2, Figs. 1–4) also contain moderately to well-preserved specimens of calcareous nannofossils. Overgrowths are notably absent on many coccoliths from Sample 577-12-2, 50 cm (Plate 3), although some coccoliths at that level are overgrown and/or etched, especially on the inner regions of the proximal side of coccolith shields (Plate 3, Fig. 3). Calcareous nannofossils at the Cretaceous/Tertiary boundary appear to be just as well, if not better, preserved than those from above and below the boundary (Plate 4, Figs. 1–4), as was observed at Site 384 by Thierstein and Okada (1979). In addition, unlike *Aragonia* from other sections of the core (Plate 2, Fig. 5), the tests of *Aragonia* from the Cretaceous/Tertiary boundary samples show fewer adhering cemented carbonate fragments and/or coccoliths (Plate 2, Fig. 6). Further examination of the carbonate trace-element data reveals that Sr/Ca ratios increase over a short interval across the Cretaceous/Tertiary boundary (Fig. 7). This provides more substantial empirical evidence on the state of preservation of the fine-fraction carbonates. During dissolution–reprecipitation of calcite, Sr ions are preferentially removed from the carbonate matrix (because the Sr partition coefficient is less than 1) so that with progressive recrystallization, cementation, or replacement the Sr/Ca ratio of the calcite should decrease (Lawrence,

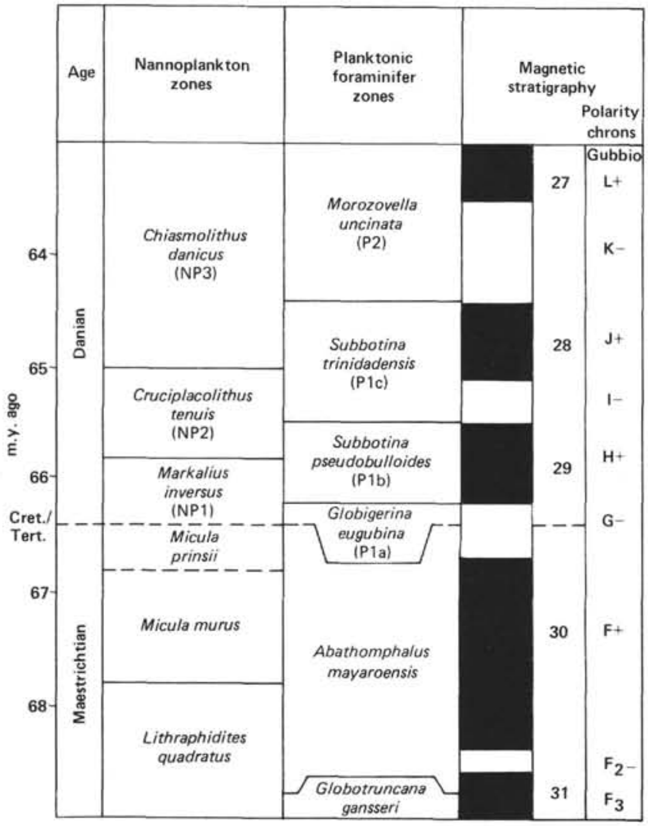

Figure 6. The Cretaceous/Tertiary boundary time scale and zonations utilized in this investigation. After van Hinte (1976), Martini (1976), Palmer (1983), Poore et al. (1983), and Berggren, Kent, and Flynn (in press). Polarity chrons are defined in Alvarez et al. (1977).

Table 3. Site 577 trace-element concentrations (<63 μm carbonate).

Core-Section (interval in cm)	% $CaCO_3$ (bulk)	Sr (ppm)	Mg (ppm)	Mn (ppm)
12-2, 49-51	90.3	1050	1010	145
12-2, 129-131	90.5	1030	950	168
12-3, 49-51	87.4	1190	1220	201
12-2, 129-131	92.8	1000	1260	139
12-4, 49-51	90.5	1030	1610	112
12-4, 89-91	87.1	1010	1820	148
12-5, 19-21	84.3	1260	2080	149
12-5, 59-61	87.1	1260	2000	149
12-5, 91-93	94.2	1640	1840	126
12-5, 108-109	94.1	1670	1760	118
12-5, 125-126	85.4	1030	1590	150
12-5, 128-130	88.4	1130	1200	101
12-5, 131-132	95.1	1080	1010	159
12-5, 144-145	95.8	1130	890	122
12-6, 39-41	95.8	1010	960	54
12-6, 99-101	96.5	940	1180	53
13-1, 59-61	95	1190	1380	79
13-1, 139-141	95	1110	1680	53
13-2, 79-81	96.4	1150	1310	49
13-3, 59-61	94.2	1140	1390	54
13-3, 139-141	93.7	1210	1570	68
13-4, 99-101	93	1230	1500	113

1971; Matter et al., 1975; Sayles and Manheim, 1975; Scholle, 1977; Brand and Veizer, 1980; Bathurst, 1981; Baker et al., 1982). However, it is difficult to imagine why the Cretaceous/Tertiary boundary carbonate would be better preserved than the carbonates in overlying sequences, considering that sedimentation rates were apparently lower, and other workers have suggested a major dissolution pulse at the boundary (e.g., Worsley, 1974). Some workers suggest that chemical preservation of

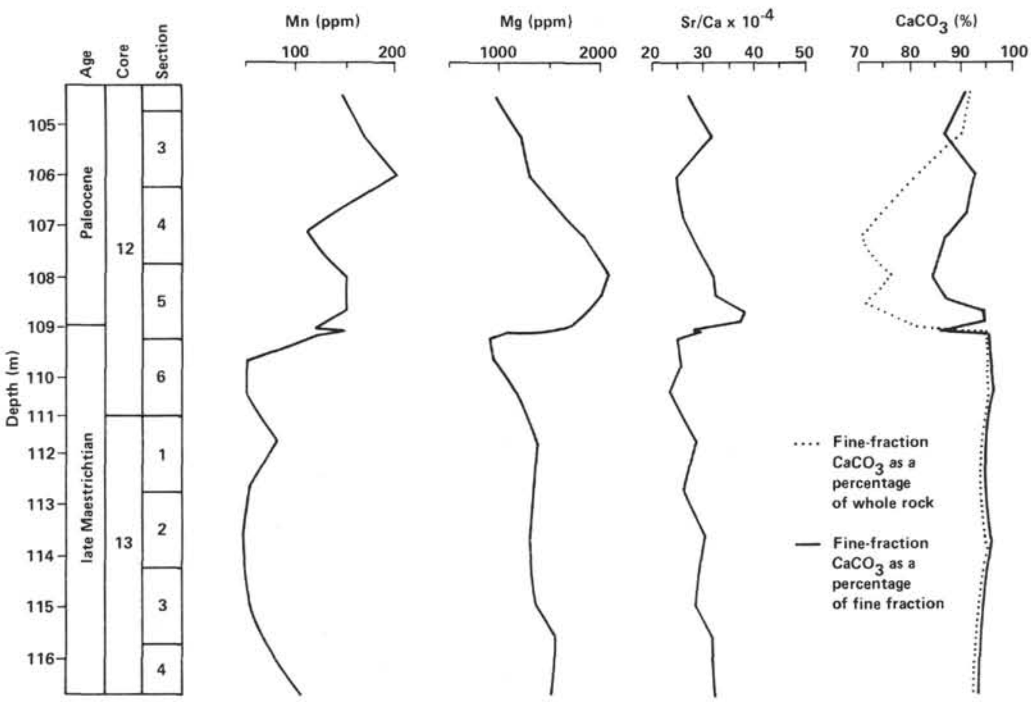

Figure 7. Manganese (Mn) and magnesium (Mg) concentrations and strontium/calcium ratios (Sr/Ca) of the fine-fraction (<63 μm) carbonates from Cores 12 and 13 of Hole 577. Fine-fraction carbonate content of whole fine-fraction and whole rock are included. The boundary is located at 109 m sub-bottom depth.

$CaCO_3$ may be enhanced if the lithology of the sediment sequence is not conducive to cementation (i.e., low porosity, high clay content, etc., Schlanger and Douglas, 1974; Matter et al., 1975). Downhole variations in preservation, therefore, may often be a function of changes in insoluble residue content. The increase in insoluble residue at the boundary represents a slight change in lithology, one which may have improved the resistance of the boundary sequence to postburial overgrowth and cementation. This is in contrast to reports of poorly preserved calcareous microfossils at some other Cretaceous/Tertiary boundary sequences (Worsley, 1974; Monechi, 1977).

An important consideration is whether or not there is any relationship between the changes in the state of preservation and the anomalies in the oxygen-isotope record. The slight enrichment in $\delta^{18}O$ at the boundary may be interpreted as improved preservation (no addition of isotopically lighter cement) rather than as a decrease in the temperature of the surface water mass in which the calcite was precipitated. Downhole changes in Sr/Ca ratios and preservation have been correlated previously with changes in oxygen-isotope records (Matter et al., 1975), whereas others have developed simple mathematical models attributing decreasing trends in $\delta^{18}O$ records through time to progressively greater diagenetic reactions with increasing age and burial depth (Killingley, 1983). Ignoring temperature effects for the moment, the somewhat anomalous $\delta^{18}O$ values of the Hole 577 boundary samples may be a function of the degree of diagenesis. If so, similar enrichments in oxygen-isotope signals at other marine boundary sequences (Site 524, Hsü et al., 1982a; Site 516, Williams et al., 1984) may also be a function of differential preservation (due to high clay content) rather than the result of real changes in oceanic temperatures.

CARBONATE ACCUMULATION RATES

Barring severe diagenesis and/or preburial dissolution, carbonate accumulation rates on the seafloor should reflect the magnitude of productivity in overlying surface waters. One would therefore expect that a postulated decrease in phytoplankton production associated with the Cretaceous/Tertiary boundary extinctions would be accompanied by a similar decrease in carbonate accumulation rates. At Hole 577 total and fine-fraction carbonate accumulation and rates decline significantly across the Cretaceous/Tertiary boundary (Table 4) (Fig. 8). Preboundary rates are stable at 1.10 g/cm^2/1000 yr., with fine-fraction carbonate accumulation contributing a major portion to the total (>99%). Just above the boundary, total carbonate accumulation rates decrease to 0.3 g/cm^2/1000 yr., with fine-fraction carbonate contributing far less as a percentage of the total (75–85%). This may imply that the decline in fine-fraction carbonate accumulation was more severe relative to the decline in foraminifer accumulation, that the recovery of foraminifer production occurred earlier than that of nannofossil (phytoplankton) production, or that current winnowing of fine-fraction carbonate occurred relative to coarse fraction.

There do not appear to be any significant variations in carbonate accumulation rates during the early Paleocene because values generally remain constant. However, accumulation rates for the entire *Cruciplacolithus tenuis* and *Markalius inversus* zones (Samples 577-12-5, 128 cm to 577-12-4, 70 cm) were determined by utilizing a single sedimentation rate of 2.9 m/m.y. This rate was determined by using the lowest datable biostratigraphic marker (first appearance datum *Chiasmolithus danicus*) available. It is probable, however, that actual sedimentation rates varied considerably over this interval. For example, the 10–20 cm of sediment lying just above the boundary may have accumulated at a much slower rate than the calculated rate of 2.9 m/m.y., by inference from the higher insoluble residue contents and the possibility that sediments higher in the *C. tenuis* Zone may have accumulated at a greater rate. This may explain why calculations reveal an increase in foraminifer accumulation rates across the boundary whereas, given the magnitude of the biotic extinctions, one might expect a decline. However, unless datable biostratigraphic markers lower than the one used to determine the average 2.9 m/m.y. rate are located, the aforementioned rate must, for the moment, be considered the best obtainable. Sedimentation rates as determined with preliminary paleomagnetic stratigraphy (Fig. 9) (Bleil, this volume) are similar to the above rates.

We believe that the magnitude of the decrease in the carbonate accumulation rate is real and not only a function of the absolute time scale used. First of all, the accumulation rate of insoluble residue (Fig. 7) does not decrease across the Cretaceous/Tertiary boundary by the same factor as the carbonate accumulation rate. Second, the insoluble residue accumulation rate decreases only gradually from Maestrichtian through Danian time.

DISCUSSION

As reported at Site 465 (Boersma and Shackleton, 1981) there appears to be little if any temperature change in surface waters across the Cretaceous/Tertiary boundary at Hole 577. The slight enrichment in the $CaCO_3$ fine-fraction $\delta^{18}O$ in Hole 577 is perhaps an artifact of preservation–diagenesis rather than a function of surface water temperature changes. However, if one were to interpret this 0.5‰ enrichment in terms of a temperature change, such an enrichment in $\delta^{18}O$ would represent a 2°C decrease in surface water temperatures at most. A second enrichment occurs in the lower part of Section 577-12-4 and may represent a slightly greater temperature decrease (3–3.5°C). Higher in the core, $\delta^{18}O$ values show significant fluctuations and are difficult to interpret. In Section 577-12-3, $\delta^{18}O$ values are slightly enriched, identical to average Maestrichtian values. However, the $\delta^{13}C$ ratios and the ratios of coarse-fraction (<63 μm) to fine-fraction carbonate over this interval are also similar to ratios in Maestrichtian sediments, indicating a possible lateral reworking of sediments through some sections at this location. The presence of poorly preserved fragments of Maestrichtian foraminifers in Section 577-12-3 is confirmation that reworking occurred.

Table 4. Site 577 accumulation rates.

Core-Section (interval in cm)	Depth (m)	Age (m.y.)	WBD (g/cm^3)	Poros.	$CaCO_3$ (%)	DBD (g/cm^3)	Sed. rate (cm/1000 yr.)	MAR	CAR	Wt. % <63 μm	FFAR (g/cm^2/1000 yr.)
12-2, 49–51	103.8	64.55	1.65	0.5	0.93	1.15	0.29	0.33	0.31	0.93	0.287
12-2, 69–71	104	64.62	1.65	0.5	0.919	1.15	0.29	0.33	0.31	0.99	0.302
12-2, 89–91	104.2	64.69	1.65	0.5	0.916	1.15	0.29	0.33	0.30	0.99	0.301
12-2, 109–111	104.4	64.76	1.65	0.5	0.938	1.15	0.29	0.33	0.31	0.97	0.302
12-2, 129–131	104.6	64.83	1.65	0.5	0.945	1.15	0.29	0.33	0.31	0.97	0.304
12-3, 9–11	104.9	64.93	1.65	0.5	0.897	1.15	0.29	0.33	0.30	0.97	0.289
12-3, 29–31	105.1	65	1.65	0.5	0.939	1.15	0.29	0.33	0.31	0.99	0.309
12-3, 49–51	105.3	65.07	1.65	0.5	0.913	1.15	0.29	0.33	0.30	0.99	0.300
12-3, 69–71	105.5	65.14	1.65	0.5	0.925	1.15	0.29	0.33	0.31	0.99	0.304
12-3, 89–91	105.7	65.21	1.65	0.5	0.879	1.15	0.29	0.33	0.29	0.99	0.289
12-3, 109–111	105.9	65.28	1.65	0.5	0.9485	1.15	0.29	0.33	0.31	0.97	0.306
12-3, 129–131	106.1	65.34	1.65	0.5	0.927	1.15	0.29	0.33	0.31	0.89	0.274
12-4, 9–11	106.4	65.45	1.65	0.5	0.954	1.15	0.29	0.33	0.32	0.86	0.272
12-4, 29–31	106.6	65.52	1.65	0.5	0.956	1.15	0.29	0.33	0.32	0.82	0.260
12-4, 49–51	106.8	65.59	1.65	0.5	0.931	1.15	0.29	0.33	0.31	0.8	0.247
12-4, 69–71	107	65.66	1.65	0.5	0.956	1.15	0.29	0.33	0.32	0.73	0.232
12-4, 89–91	107.2	65.72	1.65	0.5	0.945	1.15	0.29	0.33	0.31	0.75	0.235
12-4, 99–101	107.3	65.76	1.65	0.5	0.99	1.15	0.29	0.33	0.33	0.77	0.253
12-5, 19–21	108	66	1.65	0.5	0.931	1.15	0.29	0.33	0.31	0.8	0.247
12-5, 39–41	108.2	66.07	1.65	0.5	0.913	1.15	0.29	0.33	0.30	0.72	0.218
12-5, 59–61	108.4	66.14	1.65	0.5	0.931	1.15	0.29	0.33	0.31	0.75	0.232
12-5, 79–81	108.6	66.21	1.65	0.5	0.937	1.15	0.29	0.33	0.31	0.76	0.236
12-5, 83–85	108.64	66.22	1.65	0.5	0.93	1.15	0.29	0.33	0.31	0.83	0.256
12-5, 98–100	108.89	66.31	1.65	0.5	0.915	1.15	0.29	0.33	0.30	0.84	0.255
12-5, 108–109	108.99	66.34	1.65	0.5	0.932	1.15	0.29	0.33	0.31	0.85	0.263
12-5, 113–114	109.44	66.50	1.65	0.5	0.935	1.15	0.29	0.33	0.31	0.87	0.270
12-5, 117–119	109.09	66.38	1.65	0.5	0.895	1.15	0.29	0.33	0.30	0.91	0.270
12-5, 125–126	109.16	66.4	1.65	0.5	0.882	1.15	1	1.1	1.0	0.94	0.949
12-5, 128–130	109.19	66.40	1.65	0.5	0.888	1.15	1	1.1	1.0	0.99	1.01
12-5, 131–132	109.22	66.41	1.65	0.5	0.948	1.15	1	1.1	1.1	0.99	1.07
12-5, 134–136	109.26	66.41	1.65	0.5	0.957	1.15	1	1.1	1.1	0.99	1.08
12-5, 139–140	109.29	66.41	1.65	0.5	0.959	1.15	1	1.1	1.1	0.99	1.09
12-5, 144–145	109.35	66.42	1.65	0.5	0.96	1.15	1	1.1	1.1	0.99	1.09
12-6, 9–11	109.5	66.43	1.65	0.5	0.952	1.15	1	1.1	1.1	0.99	1.08
12-6, 19–21	109.6	66.44	1.65	0.5	0.952	1.15	1	1.1	1.1	0.99	1.08
12-6, 29–31	109.7	66.45	1.65	0.5	0.958	1.15	1	1.1	1.1	0.99	1.09
12-6, 39–41	109.8	66.46	1.65	0.5	0.961	1.15	1	1.1	1.1	0.99	1.09
12-6, 49–51	109.9	66.47	1.65	0.5	0.939	1.15	1	1.1	1.1	0.99	1.06
12-6, 59–61	110	66.48	1.65	0.5	0.948	1.15	1	1.1	1.1	0.99	1.07
12-6, 69–71	110.1	66.49	1.65	0.5	0.95	1.15	1	1.1	1.1	0.99	1.08
12-6, 79–81	110.2	66.50	1.65	0.5	0.969	1.15	1	1.1	1.1	0.99	1.10
12-6, 89–91	110.3	66.51	1.65	0.5	0.964	1.15	1	1.1	1.1	0.99	1.09
12-6, 99–101	110.4	66.52	1.65	0.5	0.952	1.15	1	1.1	1.1	0.99	1.08
12-6, 109–111	110.5	66.53	1.65	0.5	0.944	1.15	1	1.1	1.1	0.99	1.07
12-6, 119–121	110.6	66.54	1.65	0.5	0.945	1.15	1	1.1	1.1	0.99	1.07
12-6, 129–131	110.7	66.55	1.65	0.5	0.924	1.15	1	1.1	1.1	0.99	1.05
12-6, 139–141	110.8	66.56	1.65	0.5	0.944	1.15	1	1.1	1.1	0.99	1.07
12-7, 9–11	111	66.58	1.65	0.5	0.936	1.15	1	1.1	1.1	0.99	1.06
13-1, 19–21	111.4	66.62	1.65	0.5	0.946	1.15	1	1.1	1.1	0.99	1.07
13-1, 39–41	111.6	66.64	1.65	0.5	0.943	1.15	1	1.1	1.1	0.99	1.07
13-1, 59–61	111.8	66.66	1.65	0.5	0.874	1.15	1	1.1	1.0	0.99	0.991
13-1, 79–81	112	66.68	1.65	0.5	0.951	1.15	1	1.1	1.1	0.99	1.08
13-1, 99–101	112.2	66.70	1.65	0.5	0.94	1.15	1	1.1	1.1	0.99	1.07
13-1, 119–121	112.4	66.72	1.65	0.5	0.952	1.15	1	1.1	1.1	0.99	1.08
13-1, 139–141	112.6	66.74	1.65	0.5	0.9538	1.15	1	1.1	1.1	0.99	1.08
13-2, 19–21	112.9	66.77	1.65	0.5	0.904	1.15	1	1.1	1.0	0.99	1.02
13-2, 39–41	113.1	66.79	1.65	0.5	0.963	1.15	1	1.1	1.1	0.99	1.09
13-2, 59–61	113.3	66.81	1.65	0.5	0.961	1.15	1	1.1	1.1	0.99	1.09
13-2, 79–81	113.5	66.83	1.65	0.5	0.945	1.15	1	1.1	1.1	0.99	1.07
13-2, 99–101	113.7	66.85	1.65	0.5	0.949	1.15	1	1.1	1.1	0.99	1.08
13-2, 119–121	113.9	66.87	1.65	0.5	0.948	1.15	1	1.1	1.1	0.99	1.07
13-2, 139–141	114.1	66.89	1.65	0.5	0.95	1.15	1	1.1	1.1	0.99	1.08
13-3, 19–21	114.4	66.92	1.65	0.5	0.94	1.15	1	1.1	1.1	0.99	1.07
13-3, 39–41	114.6	66.94	1.65	0.5	0.953	1.15	1	1.1	1.1	0.99	1.08
13-3, 59–61	114.8	66.96	1.65	0.5	0.946	1.15	1	1.1	1.1	0.99	1.07
13-3, 79–81	115	66.98	1.65	0.5	0.974	1.15	1	1.1	1.1	0.99	1.10
13-3, 99–101	115.2	67.00	1.65	0.5	0.909	1.15	1	1.1	1.0	0.99	1.03
13-3, 119–121	115.4	67.02	1.65	0.5	0.964	1.15	1	1.1	1.1	0.99	1.09
13-3, 139–141	115.6	67.04	1.65	0.5	0.951	1.15	1	1.1	1.1	0.99	1.08
13-4, 19–21	115.9	67.07	1.65	0.5	0.924	1.15	1	1.1	1.1	0.99	1.05
13-4, 39–41	116.1	67.09	1.65	0.5	0.941	1.15	1	1.1	1.1	0.99	1.07
13-4, 59–61	116.3	67.11	1.65	0.5	0.95	1.15	1	1.1	1.1	0.99	1.08
13-4, 79–81	116.5	67.13	1.65	0.5	0.948	1.15	1	1.1	1.1	0.99	1.07
13-4, 99–101	116.7	67.15	1.65	0.5	0.949	1.15	1	1.1	1.1	0.99	1.08
13-4, 119–121	116.9	67.17	1.65	0.5	0.928	1.15	1	1.1	1.1	0.99	1.05
13-4, 139–141	117.1	67.19	1.65	0.5	0.952	1.15	1	1.1	1.1	0.99	1.08

Note: WBD = wet bulk density, DBD = dry bulk density, MAR = mass accumulation rate (g/cm^2/1000 yr.), CAR = carbonate accumulation rate (g/cm^2/1000 yr.), FFAR = fine fraction accumulation rate (g/cm^2/1000 yr.).

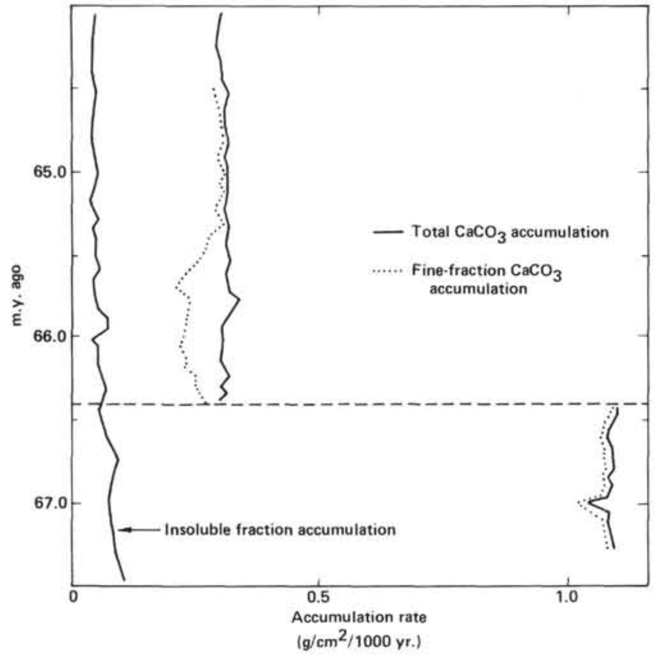

Figure 8. Total carbonate, fine-fraction carbonate, and insoluble fraction accumulation rates prior to and following the Cretaceous/Tertiary boundary.

Nonetheless, overall $\delta^{18}O$ values in uncontaminated Danian sections at Hole 577 tend to be lighter than Maestrichtian values. Because preservation changes relatively little, this implies a slight warming in surface waters. A slight cooling was apparently recorded by the whole rock values at Site 47.2 and by planktonic foraminifers from Site 465 where the $\delta^{18}O$ values of Danian foraminifers are somewhat heavier (Fig. 4) than the values of their Maestrichtian counterparts. Isotopic paleotemperature estimates for surface waters at the studied sites average near 15–18°C for the Maestrichtian and 14–18°C for the Danian. These temperatures appear to be rather cool for the estimated paleolatitude of about 15°N (Fig. 8) (Lancelot and Larson, 1975), but are in line with those calculated from other published data (Boersma and Shackleton, 1981).

The benthic oxygen-isotope stratigraphy from Site 465 and Hole 577 suggests that bottom water temperatures did not change systematically from the Maestrichtian to the Danian. At Site 465, $\delta^{18}O$ values of *Bulimina* showed variations amounting to about 4°C in paleotemperature estimates. The range of $\delta^{18}O$ values of *Aragonia* in Hole 577 was somewhat less. Because different species of benthic foraminifers were analyzed at each location, we can only speculate on the relative bottom-water temperatures of these two sites. However, considering the relatively small difference (0.5‰) in $\delta^{18}O$ between these two sections, it may be reasonable to assume that bottom-water temperatures at Sites 465 and 577 were very similar if not equal. The estimated isotopic paleotemperatures of deep water at the sites are between 8 and 12°C both above and below the Cretaceous/Tertiary boundary. These values fall within the range for shallow intermediate waters (< 1500 m) determined for inoceramids for the Late Cretaceous at other DSDP sites (Saltzman and Barron, 1982). There appears to have been relatively little change in the vertical temperature gradient across the Cretaceous/Tertiary boundary at either Site 465 or 577, but $\delta^{18}O$ values of *Aragonia* from Hole 577 suggest cooling across the boundary whereas $\delta^{18}O$ values of *Bulimina* from Site 465 apparently record a brief warming episode. The estimated paleodepths of Sites 465 and 577 are about 1500 and 2400 m, respectively (using subsidence curves and assumptions of Thiede et al., 1982). The estimated paleotemperatures at Hole 577 appear to be too warm for the deeper paleodepth.

The negative $\delta^{13}C$ shift of about 1.0‰ recorded in the fine-fraction carbonate at the Cretaceous/Tertiary boundary at Hole 577 has been found in varying magnitudes at nearly every Cretaceous/Tertiary boundary sequence studied (e.g., Arthur et al., 1979; Scholle and Arthur, 1980; Hsü et al., 1982a; Perch-Nielsen et al., 1982). The negative shift detected in our data from Hole 577 occurs within a few centimeters of the Cretaceous/Tertiary boundary determined by calcareous nannofossil stratigraphy (Monechi, this volume) and the major iridium spike and highest Ir/Fe ratio (Michel et al., this volume). The close correspondence of the $\delta^{13}C$ anomaly and the iridium anomaly in most other sections (Hsü et al., 1982a; Zachos et al., unpubl. data) across the Cretaceous/Tertiary boundary suggest that the $\delta^{13}C$ shift is an excellent stratigraphic marker for the boundary (barring significant hiatuses). Some investigators have interpreted this anomaly to represent a decrease in oceanic surface water phytoplankton production (Boersma et al., 1979; Boersma and Shackleton, 1981; Arthur and Dean, 1982; Hsü et al., 1982a, b). While a number of authors have speculated on the cause of the catastrophy that brought about the extinctions and what effects the event and accompanying phytoplankton extinctions may have had on global climate, few have attempted to quantify the magnitude of the decline in marine productivity or its duration. Boersma and Shackleton (1981) and Hsü et al. (1982a) determined the $\delta^{13}C$ of benthic foraminifers as well as measuring the $\delta^{13}C$ of corresponding planktonic organisms, recognizing that the abrupt decline in $\delta^{13}C$ across the boundary might only have been a surface-water phenomenon. Benthic foraminifers tend to record the $\delta^{13}C$ of deep water (Woodruff et al., 1980, Belanger et al., 1981; Savin and Yeh, 1981) although, as mentioned earlier, some interspecies fractionation effects exist. By comparing the benthic and planktonic foraminifer carbon-isotope records, Boersma and Shackleton (1981) were able to establish rough estimates of surface to deep-water carbon-isotope gradients prior to and following the Cretaceous/Tertiary boundary. Surface to deep-water carbon-isotope gradients of the modern oceans have been correlated with nutrient gradients (Broecker, 1974, Broecker and Peng, 1982) and dissolved oxygen or apparent oxygen utilization (Kroopnick et al., 1970; Williams et al., 1977; Kroopnick, 1974, 1980) and, hence, with primary productivity in surface waters and carbon oxidation in deep-water masses. Therefore, variations in primary productivity and consequent transfer and oxidation of organic matter in deeper waters should be reflected in

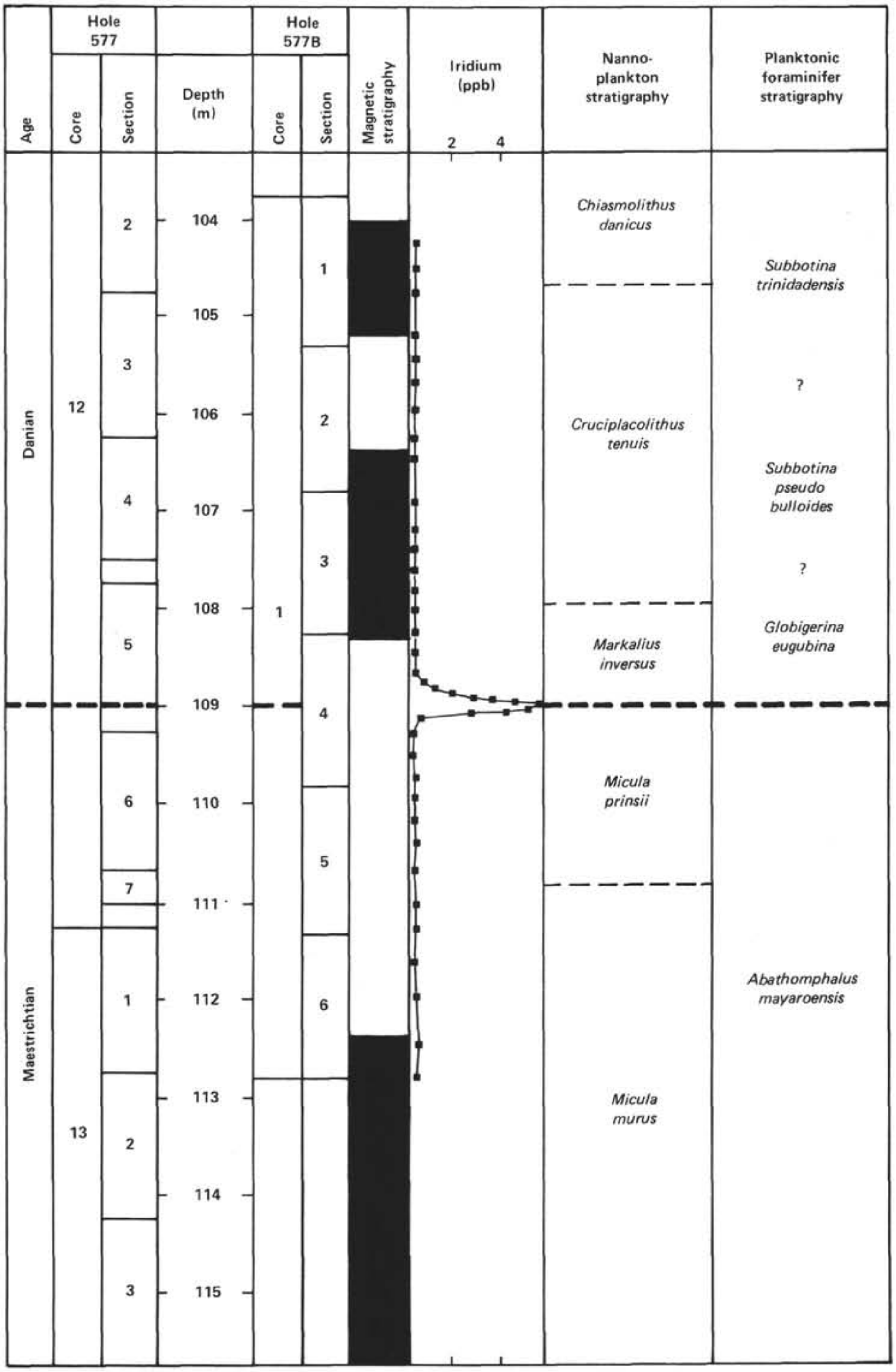

Figure 9. Correlation between Holes 577 and 577B showing magnetic stratigraphy (Bleil, this volume) and iridium concentrations as measured in Hole 577B (Michel et al., this volume). Cretaceous/Tertiary boundary was chosen at both holes on the basis of calcareous nannofossil biostratigraphy (Monechi, this volume). The nannoplankton and planktonic foraminifer stratigraphies in the right two columns are those of Hole 577.

changes in the surface to deep water $\delta^{13}C$ gradients inferred from calcareous planktonic and benthic organisms. From the Maestrichtian to the Danian at Site 465, there was a decrease in the surface to deep water $\delta^{13}C$ gradient from 1.5 to 0‰ which was interpreted to represent an almost complete cessation of total dissolved CO_2 utilization for organic carbon production in surface waters (Boersma and Shackleton, 1981). The change in Maestrichtian to Danian surface- to deep-water carbon-isotope gradients at Hole 577, as the difference between the $\delta^{13}C$ of fine-fraction carbonate and of the benthic foraminifer *Aragonia*, was similar in magnitude to the change measured at Site 465 (Fig. 4). The decrease in the $\delta^{13}C$ gradient of 1.5‰ at Site 465, however, was a direct result of the decrease in planktonic carbon-isotope ratios because the carbon-isotope values of the benthic foraminifer *Bulimina* remained more or less constant. The change in surface to deep gradients at Hole 577 was partially a function of both an approximate 0.8‰ enrichment in benthic carbon-isotope values and a decrease of 0.8 to 1.0‰ in fine-fraction $\delta^{13}C$. This reduction of the surface to deep $\delta^{13}C$ gradient at the Cretaceous/Tertiary boundary is similar in some respects to the reduction of the $\delta^{13}C$ gradients in some freshwater lakes during the summer to winter transition when surface water productivity declines and summer thermal stratification is removed by vertical mixing (e.g., McKenzie, 1982). Following a fairly abrupt decline in surface organic productivity at the Cretaceous/Tertiary boundary that might have accompanied extinction of the majority of calcareous nannoplankton species, the flux of organic matter to deep-water masses would rapidly decrease. The amount of isotopically light CO_2 released from the decaying detritus would therefore decrease and $\delta^{13}C$ values for Danian deep-water masses may be more positive relative to those of the Late Cretaceous.

Further upcore at Hole 577, benthic $\delta^{13}C$ values decrease, reaching preboundary levels within the *Cruciplocolithus tenuis* zone. In addition, surface- to deep-carbon isotope gradients also return to preboundary levels by 2 m.y. following the event. If we assume that a positive surface to deep $\delta^{13}C$ gradient is produced by normally operating transfer mechanisms, such as the preferred extraction of isotopically light carbon from surface water in the organic flux to deep waters resulting from higher primary productivity, then these data may be interpreted to suggest that primary production recovered to near preboundary levels about 2 m.y. after the extinction event. However, the equilibrium levels of both surface and deep $\delta^{13}C$ were apparently much lighter in the Danian than in the Maestrichtian, perhaps because the overall rate of organic carbon burial was still somewhat lower in the Danian than during the late Maestrichtian (e.g., Scholle and Arthur, 1980) following the Cretaceous/Tertiary "event." The lighter average $\delta^{13}C$ values would therefore be a whole-reservoir signal.

On the basis of the change in planktonic foraminifer/nannofossil ratios, it appears that the rate of production of calcareous nannofossils decreased relative to the production of planktonic foraminifers or that planktonic foraminifers were able to recover much more quickly. Berger (1976), however, suggested that increases in the foraminifer/nannofossil ratio were the result of increased winnowing. This seems unlikely given the thickness of the section with higher foraminifer ratios (200 cm) and the absence of apparent current-induced laminations or other primary sedimentary structures indicative of current action. Foraminifers have a greater depth stratification than nannofossils, which generally inhabit only the photic zone, and as a group may have been able to maintain higher levels of productivity. The transition from nannofossil to relatively foraminifer-rich sediment occurs gradually across the Cretaceous/Tertiary boundary. Coarse fraction percentages increase from less than 1% to as much as 24% of the total sediment weight over a 60-cm interval above the boundary (Table 1). This suggests that the inferred productivity decrease may not have occurred instantly, geologically speaking, or that bioturbation mixed out the originally sharp change (e.g., Thierstein and Okada, 1979). Perch-Neilsen et al. (1982) and Hsü et al. (1982a) have presented evidence indicating that the extinction of calcareous nannoplankton may have occurred over a longer period than previously believed. However, in light of the sudden shift in carbon-isotope records across the boundary in the apparently continuous pelagic sequence at Site 577, it would be difficult to suggest that the decline in productivity was a slow and gradual process. It must have occurred in a period of less than 28,000 yr.

CONCLUSIONS

On the basis of available biostratigraphic and geochemical evidence (Monechi, this volume; Michel et al., this volume), we assume that the pelagic carbonate sequence at Hole 577 is continuous across the Cretaceous/Tertiary boundary. Our trace-element and SEM studies of closely spaced samples across the Cretaceous/Tertiary boundary suggest that there are relatively small changes in preservation of calcareous microplankton and nannoplankton assemblages across the boundary. Oxygen-isotope determinations of the calcareous fine-fraction (representing surface-water masses) and benthic foraminifers in Hole 577 suggest relatively little temperature change in surface or deep-water masses across the boundary. Similar results were obtained in studies of DSDP Site 47.2 on the Shatsky Rise and Site 465 on nearby Hess Rise. The $\delta^{13}C$ gradient, inferred from analyses of planktonic and benthic calcareous groups, decreased abruptly at the Cretaceous/Tertiary boundary in conjunction with nannofossil and foraminifer extinctions and an increase in Ir concentrations and the Ir/Fe ratio. We attribute the change in the $\delta^{13}C$ gradient to a sudden decrease in surface productivity associated with the extinction event. Further substantiation of this is given by a significant reduction of carbonate accumulation rates across the Cretaceous/Tertiary boundary at Hole 577 and other localities without apparent significant changes in carbonate preservation. The decline in carbonate production/accumulation apparently lasted at least 2 m.y. The relationship to a postulated meteoritic impact, however, is not clear. Previously hypothesized temperature and carbonate preservational changes at the boundary are not evident at Pacific DSDP sites analyzed so far. The mechanism(s) for the extinctions and for decreased plankton productivity at the Cretaceous/Tertiary boundary remain(s) obscure.

ACKNOWLEDGMENTS

The authors would like to thank Hans Thierstein, Nick Shackleton, James Kennett, and Audrey Wright for reviewing this manuscript and offering helpful criticism and Maria Burdett for drafting original figures. This work was supported by NSF Grant EAR-8306561.

REFERENCES

Adelseck, C. G., Geehan, G. W., and Roth, P. H., 1973. Experimental evidence for the selective dissolution and overgrowth of calcareous nannofossils during diagenesis. *Geol. Soc. Am. Bull.*, 84(8): 2755–2762.

Alvarez, L. W., Alvarez, W., Asaro, F., and Michel, H., 1980. Extraterrestrial cause for the Cretaceous-Tertiary extinctions. *Science*, 208:1095–1108.

Alvarez, W., Alvarez, L. W., Asaro, F., and Michel, H. V., 1982. Current status of the impact theory for the terminal Cretaceous extinction. *In* Silver, L. T., and Shultz, P. H. (Eds.), *Geologic Implications of Impacts of Large Asteroids and Comets on the Earth*. Geol. Soc. Am. Spec. Pap., 190:305–315.

Alvarez, W., Arthur, M., Fischer, A. G., Lowrie, W., Giovanni, N., Premoli Silva, I., and Roggenthen, W. N., 1977. The upper Cretaceous-Paleocene magnetic stratigraphy at Gubbio, Italy. *Geol. Soc. Am. Bull.*, 88:367–389.

Arthur, M. A., and Dean, W. E., 1982. Changes in deep ocean circulation and carbon cycling at the Cretaceous-Tertiary boundary *In* Herschmen, A., (Ed.), *Abstracts of Papers of the 148th Natl. Meeting of the Amer. Assoc. for the Advance. of Sci.* AAAS Public., No. 82-2, p. 48. (Abstract)

Arthur, M. A., Scholle, P. A., and Hasson, P., 1979. Stable isotopes of oxygen and carbon in carbonates from Sites 398 and 116 of the Deep Sea Drilling Project. *In* Sibuet, J.-C. Ryan, W. B. F., et al., *Init. Repts. DSDP*, 47, Pt. 2: Washington (U.S. Govt. Printing Office), 477–492.

Baker, P. A., Gieskes, J. M., and Elderfield, H., 1982. Diagenesis of carbonates in deep sea sediments—evidence from Sr/Ca ratios and interstitial dissolved Sr data. *J. Sediment. Petrol.*, 52(1):0071–0082.

Bathurst, R. G. C., 1981. *Carbonate Sediments and Their Diagenesis*: Amsterdam (Elsevier).

Belanger, P. E., Curry, W. B., and Matthews, R. K., 1981. Core-top evaluation of benthic foraminiferal isotopic ratios for paleo-oceanographic interpretations. *Paleogeogr. Paleoclimatol., Paleoecol.*, 33:205–220.

Berger, W. H., 1975. Deep sea carbonates. Dissolution profiles from foraminiferal preservation. *In* Sliter, W. V., Bé, A. W. H., and Berger, W. H., (Eds.), *Dissolution of Deep-Sea Carbonate*. Spec. Publ. Cushman Found. Foraminiferal Res., 13:82–86.

________, 1976. Biogenous deep sea sediments: Production, preservation, and interpretation. *In* Riley, J. P., and Chester, R. (Eds.) *Treatise on Chemical Oceanography* (Vol. 5): New York (Academic Press), 265–388.

Berggren, W. A., Kent, D. V., and Flynn, J. J., in press. Paleogene geochronology and chronostratigraphy. *In Geochronology and the Geological Record*: London (Geol. Soc. London).

Boersma, A., and Shackleton, N. J., 1981. Oxygen and carbon isotope variations and planktonic-foraminifer depth habitats, Late Cretaceous to Paleocene, Central Pacific. *In* Thiede, J., Vallier, T. L., et al., *Init. Repts. DSDP*, 62: Washington (U.S. Govt. Printing Office), 513–526.

Boersma, A., Shackleton, N. J., Hall, M., and Given, Q., 1979. Carbon and oxygen isotope records at DSDP Site 384 (North Atlantic) and some Paleocene paleotemperatures and carbon isotope variations in the Atlantic Ocean. *In* Tucholke, B. E., Vogt, P. R., et al., *Init. Repts. DSDP*, 43: Washington (U.S. Govt. Printing Office), 695–717.

Bramlette, M. N., 1965. Massive extinctions of biota at the end of Mesozoic time. *Science*, 148:1696–1699.

Brand, U., and Veizer, J., 1980. Chemical diagenesis of a multicomponent carbonate system—1: Trace elements. *J. Sediment. Petrol.*, 50:1219–1236.

Broecker, W. S., 1974. *Chemical Oceanography*: New York (Harcourt Brace Jovanovich).

Broecker, W. S., and Peng, T.-H., 1982. *Tracers in the Sea*: New York (Lamont-Doherty Geological Observatory, Columbia University).

Douglas, R., and Savin, S., 1971. Isotopic analyses of planktonic foraminifera from the Cenozoic of the Northwest Pacific, Leg 6. *In* Fischer, A. G., Heezen, B. C., et al., *Init. Repts. DSDP*, 6: Washington (U.S. Govt. Printing Office), 1123–1127.

Douglas, R., and Woodruff, F., 1981. Deep sea benthic Foraminifera. *In* Emiliani, C. (Ed.), *The Oceanic Lithosphere*: New York (Wiley), pp. 1233–1327.

Emiliani, C., Kraus, E. B., and Shoemaker, E. M., 1981. Sudden death at the end of the Mesozoic. *Earth Planet. Sci. Lett.*, 55: 317–334.

Firstbrook, P. L., Funnel, B. M., Hurley, A. M., and Smith, A. G., 1979. Paleoceanic reconstructions 160-0 Ma. Univ. of California, *National Science Foundation National Ocean Sediment Coring Program*, p. 22.

Fischer, A. G., and Arthur, M. A., 1977. Secular variations in the pelagic realm. *Spec. Publ. Soc. Econ. Paleontol. Mineral.*, 25:19–50.

Hofker, J., 1978. Analysis of a large succession of samples through the upper Maestrichtian and the lower Tertiary of drill Hole 47.2, Shatsky Rise, Pacific, DSDP. *J. Foraminiferal Res.*, 8:46–75.

Hsü, K. J., 1980. Terrestrial catastrophe by cometary impact at the end of the Cretaceous. *Nature*, 285:201–203.

Hsü, K. J., He, Q., McKenzie, J. A., Weissert, H., Perch-Nielsen, K., Oberhansli, H., Kelts, K., LaBrecque, J., Tauxe, L., Krahenbuhl, U., Percival, S. F., Wright, R., Karpoff, A. M., Petersen, N., Tucker, P., Poore, R. Z., Gombod, A. M., Pisciotto, K., Carman, M. F., and Schreiber, E., 1982a. Mass mortality and its environmental and evolutionary consequences. *Science*, 216:249–256.

Hsü, K. J., McKenzie, J. A., He, Q. X., 1982b. Terminal Cretaceous environmental and evolutionary changes. *In* Silver, L. T., and Shultz, P. H., (Eds.), *Geological Implications of Large Asteriods and Comets on the Earth*. Geol. Soc. Am. Spec. Pap. 190:317–328.

Keigwin, L. D., 1980. Paleoceanographic change in the Pacific at the Eocene-Oligocene boundary. *Nature*, 287:722–725.

Killingley, J. S., 1983. Effects of diagenetic recrystallization on $^{18}O/^{16}O$ values of deep sea sediments. *Nature*, 301:594–597.

Kroopnick, P., 1974. Modeling the dissolved O_2–CO_2–^{13}C system in the eastern equatorial Pacific *Deep Sea Res.*, 21:211–229.

________, 1980. The distribution of ^{13}C in the Atlantic Ocean. *Earth Planet. Sci. Lett.*, 49:469–484.

Kroopnick, P., Deuser, W. G., Craig, H., 1970. Carbon-13 measurements on dissolved inorganic carbon at the North Pacific (1969) GEOSECS station. *J. Geophys. Res.*, 75:7668–7671.

Lancelot, Y., and Larson, R. L., 1975. Sedimentary and tectonic evolution of Northwestern Pacific. *In* Larson, R. L., Moberly, R., et al., *Init. Repts. DSDP*, 32: Washington (U.S. Govt. Printing Office), 925–940.

Lawrence, J. R., 1971. Interstitial water studies, Leg 15-Stable oxygen and carbon isotope variations in water, carbonates, and silicates from the Venezuela Basin (Site 149) and the Aves Rise (Site 148). *In* Heezen, B. C., MacGregor, I. D., et al., *Init. Repts. DSDP*, 20: Washington (U.S. Govt. Printing Office), 891–900.

McKenzie, J. A., 1982. Carbon-13 cycle in Lake Greifen: a model for restricted ocean basins. *In* Schlanger, S. O., and Cita, M. B. (Eds.), *Nature and Origin of Cretaceous Carbon Rich Facies*: New York (Academic Press), pp. 197–208.

McLean, D. M., 1980. Terminal Cretaceous catastrophe. *Nature*, 287: 760.

________, 1982. Flood basalt volcanism and global extinctions at the Cretaceous-Tertiary transition. *In* Herschmen, A. (Ed.), *Abstracts of Papers of the 148th National Meeting of the Amer. Assoc. for the Advance. of Sci.* AAAS Publ., No. 82-2, p. 47. (Abstract)

Martini, E., 1976. Cretaceous to Recent calcareous nannoplankton from the Central Pacific Ocean (DSDP Leg 33). *In* Schlanger, S. O., Jackson, E. D., et al., *Init. Repts. DSDP*, 33: Washington (U.S. Govt. Printing Office), 383–423.

Matter, A., Douglas, R. G., and Perch-Nielsen, K., 1975. Fossil preservation, geochemistry and diagenesis of pelagic carbonates from Shatsky Rise, N.W. Pacific. *In* Larson, R. L., Moberly, R., et al., *Init. Repts. DSDP*, 32: Washington (U.S. Govt. Printing Office), pp. 891–922.

Monechi, S., 1977. Upper Cretaceous and Early Tertiary nannoplankton from the Scaglia Umbra Formation (Gubbio, Italy). *Riv. Ital. Paleontol.*, 83:754–802.

Müller, G., and Gastner, M., 1971. The "Karbonate Bombe," a simple device for the determination of the carbonate content in sediments, soils, and other materials. *Neves Jahrb. Mineral. Monatsh.*, 10: 466–469.

Officer, C. B., and Drake, C. L., 1983. The Cretaceous-Tertiary transition. *Science*, 219:1383–1390.

Palmer, A. R., 1983. The decade of North American geology, 1983 geologic time scale. *Geology*, 11:503–504.

Perch-Nielsen, K., McKenzie, J., and He, Q., 1982. Biostratigraphy and isotope stratigraphy and the "Catastrophic" extinction of calcareous nannoplankton at the Cretaceous/Tertiary boundary. *In*

Silver, L. T., and Schultz, P. H. (Eds.), *Geological Implications of Impacts of Large Asteriods and Comets on the Earth*. Geol. Soc. Am. Spec. Pap., 190:353–371.

Poore, R. A., Tauxe, L., Percival, S. F., LaBrecque, J. L., Wright, R., Petersen, N. P., Smith, C. C., Tucker, P., and Hsü, K. J., 1983. Late Cretaceous-Cenozoic magnetostratigraphic and biostratigraphic correlations of the South Atlantic Ocean: DSDP Leg 73. *Paleogeogr., Paleoclimatol., Paleoecol.*, 42:127–148.

Roth, P. H., and Berger, W. H., 1975. Distribution and dissolution of coccoliths in the South and Central Pacific. *In* Sliter, W. V., Bé, A. W. H., and Berger, W. H. (Eds.), *Dissolution of Deep Sea Carbonates*. Spec. Publ. Cushman Found. Foraminiferal Res. 13: 87–113.

Saltzman, E. S., Barron, E. J., 1982. Deep circulation in the Late Cretaceous; oxygen isotope paleotemperatures from *Inocermus* remains in DSDP cores. *Paleogeogr., Paleoclimatol., Paleoecol.*, 40: 167–181.

Savin, S. M., and Yeh, H. W., 1981. Stable isotopes in ocean sediments. *In* Emiliani, C. (Ed.), *The Sea* (Vol. 7): New York (Wiley-Interscience), 1521–1554.

Sayles, F. L., and Manheim, F. T., 1975. Interstitial solutions and diagenesis in deeply buried marine sediments: Results from the Deep Sea Drilling Project. *Geochim. Cosmochim. Acta.*, 39:103–127.

Schlanger, S. O., and Douglas, R. G., 1974. The pelagic ooze-chalk-limestone transition and its implications for marine stratigraphy. *In* Hsü, K. J., and Jenkyns, H. C. (Eds.), *Pelagic Sediments on Land and under the Sea*. Int. Assoc. Sed. Spec. Public., 1:177–210.

Scholle, P. A., 1977. Chalk diagenesis and its relation to petroleum exploration: Oil from chalks a modern miracle? *Am. Assoc. Pet. Geol. Bull.*, 61:982–1009.

Scholle, P. A., and Arthur, M. A., 1980. Carbon isotope fluctuations in Cretaceous pelagic limestones; potential stratigraphic and petroleum exploration tool. *Am. Assoc. Pet. Geol. Bull.*, 64:67–87.

Silver, L. T., and Schultz, P. H. (Eds.), 1982. Geological implications of impacts of large asteroids and comets on the Earth. *Geol. Soc. Am. Spec. Pap.*, 190.

Tappan, H., 1968. Primary production, isotopes, extinctions and the atmosphere. *Paleogeogr., Paleoclimatol., Paleoecol.*, 4:187–210.

Thiede, J., Dean, W. E., and Claypool, G. E., 1982. Oxygen deficient depositional environments in the Mid-Cretaceous tropical to subtropical Pacific Ocean. *In* Schlanger, S. O., and Cita, M. B. (Eds.), *Nature and Origin of Cretaceous Carbon-Rich Facies*: New York (Academic Press), pp. 79–100.

Thierstein, H. R., 1980. Selective dissolution of Late Cretaceous and earliest Tertiary calcareous nannofossils: Experimental evidence. *Cretaceous Res.*, 2:165–176.

_______, 1981. Late Cretaceous nannoplankton and the Cretaceous/Tertiary boundary. *Soc. Econ. Paleontol. Mineral.*, 32:355–394.

_______, 1982. Terminal Cretaceous plankton extinctions: A critical assessment. *In* Silver, L. T., and Schultz, P. H. (Eds.), *Geological Implications of Impacts of Large Asteriods and Comets on the Earth*. Geol. Soc. Am. Spec. Paper, 190:385–400.

Thierstein, H. R., and Okada, H., 1979. The Cretaceous/Tertiary boundary event in the North Atlantic. *In* Tucholke, B. E., Vogt, P. R., et al., *Init. Repts. DSDP*, 43: Washington (U.S. Govt. Printing Office), 601–616.

Thunell, R. C., 1982. Carbonate dissolution and abyssal hydrography in the Atlantic Ocean. *Mar. Geol.*, 47:165–180.

Toon, O. B., Pollack, J. B., Ackerman, T. P., Turco, R. P., McKay, C. P., and Liu, M. S., 1982. Evolution of an impact-generated dust cloud and its effects on the atmosphere. *In* Silver, L. T., and Schultz, P. H. (Eds.), *Geological Implications of Impacts of Large Asteroids and Comets on the Earth*. Geol. Soc. Am. Spec. Pap., 190:187–200.

van Hinte, J. E., 1976. A Cretaceous time scale. *Am. Assoc. Petrol. Geol. Bull.*, 60:498–516.

Veizer, J., 1978. Simulation of limestone diagenesis—a model based on strontium depletion: Discussion. *Can. J. Earth. Sci.*, 15: 1683–1686.

Vogt, P. R., 1972. Evidence for global synchronism in mantle plume convection, and possible significance for geology. *Nature*, (*London*) 240:338–342.

Williams, D. F., Healy-Williams, N., Thunell, R. C., and Leventer, A., 1983. Detailed stable isotope and carbonate records from the late Maestrichtian early Paleocene section of Site 516F (Leg 72) including the Cretaceous/Tertiary boundary. *In* Barker, P. F., Carlson, R. L., Johnson, D. A., et al., *Init. Repts. DSDP*, 72: Washington (U.S. Govt. Printing Office), 921–930.

Williams, D. F., Sommer, M. A., and Bender, M. L., 1977. Carbon isotopic composition of recent planktonic foraminifera of the Indian Ocean. *Earth Planet. Sci. Lett.*, 36:391–403.

Woodruff, F., Savin, S., and Douglas, R., 1980. Biological fractionation of oxygen and carbon isotopes by recent benthic foraminifera. *Mar. Micropaleontol.*, 5:3–11.

Worsley, T., 1974. The Cretaceous-Tertiary boundary event in the ocean. *Soc. Econ. Paleontol. Mineral., Spec. Publ.*, 20:94–125.

Zoller, W. H., Parrington, J. R., and Phelan Kotra, J. M., 1983. Iridium enrichment in airborne particles from Kilauea volcano: January 1983. *Science*, 222:1118–1121.

Date of Initial Receipt: 17 January 1984
Date of Acceptance: 17 August 1984

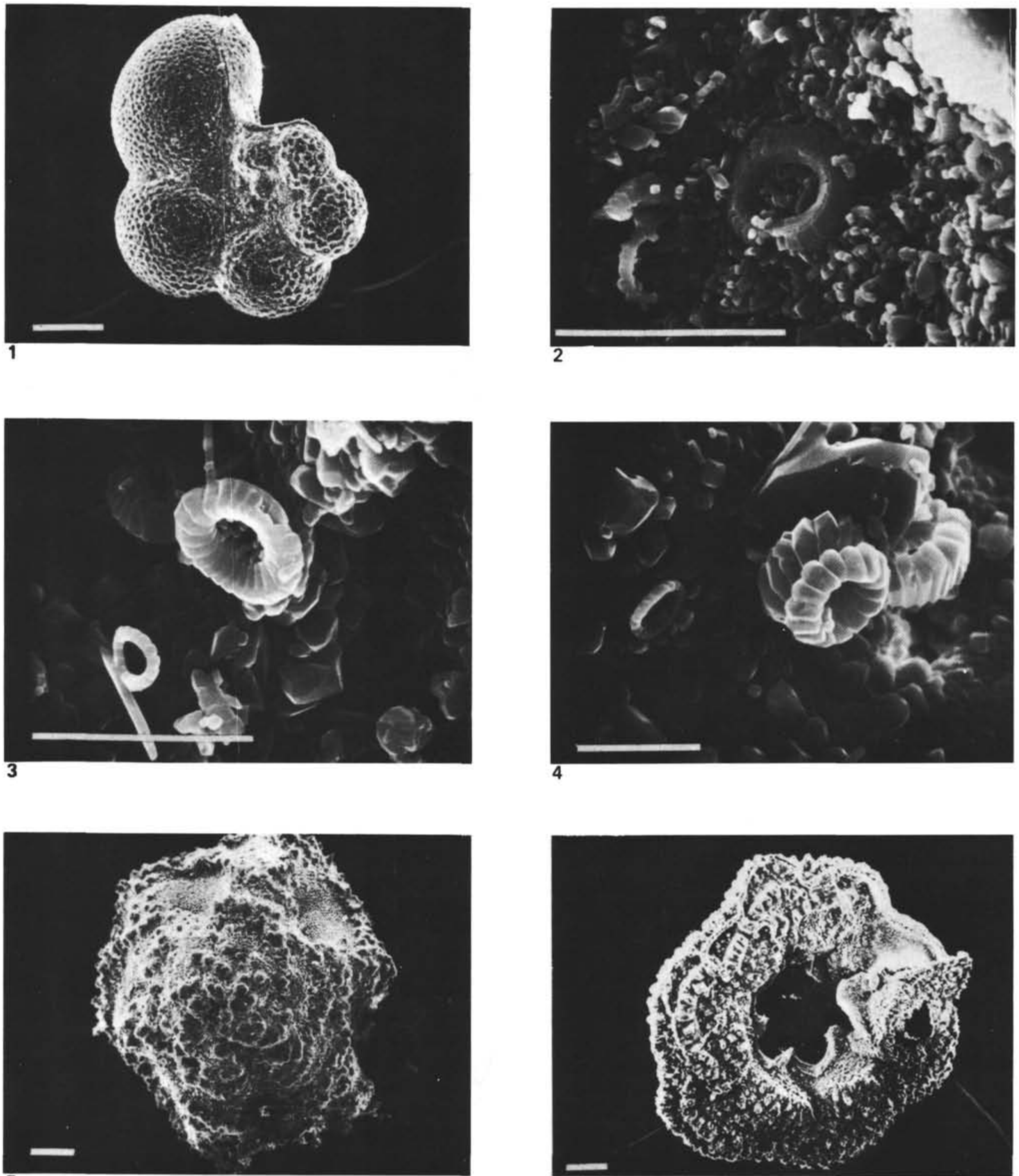

Plate 1. Site 47.2. **1.** *Gioborotalia trinidadensis* (Bolli), Sample 47.2-11-2, 45 cm. Bar = 100 μm. **2.** Danian calcareous nannofossil ooze, Sample 47.2-11-2, 45 cm. Bar = 10 μm. **3, 4.** Maestrichtian calcareous nannofossils, Sample 47.2-12-1, 28 cm. Bar = 10 μm. **5, 6.** Spiral and umbilical views of *Globotruncana contusa* (Cushman), Sample 47.2-11-1, 28 cm. Bar = 100 μm.

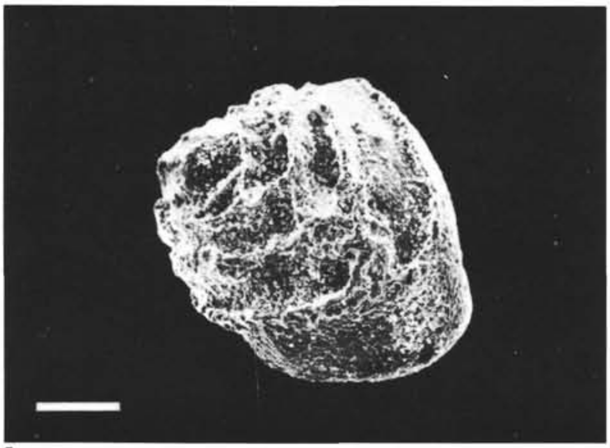
1


2

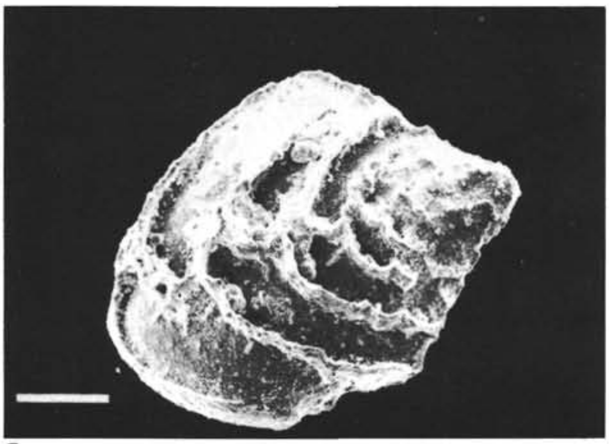
3

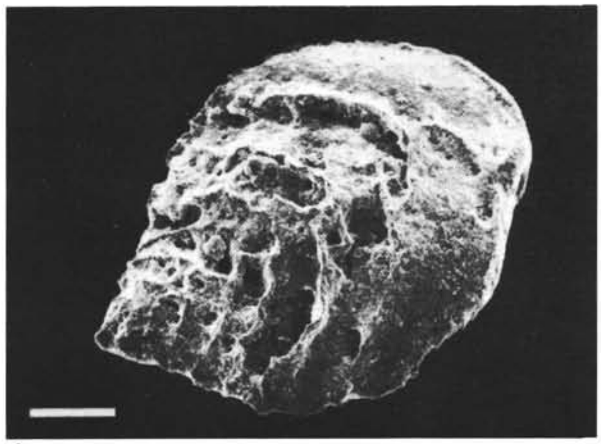
4


5

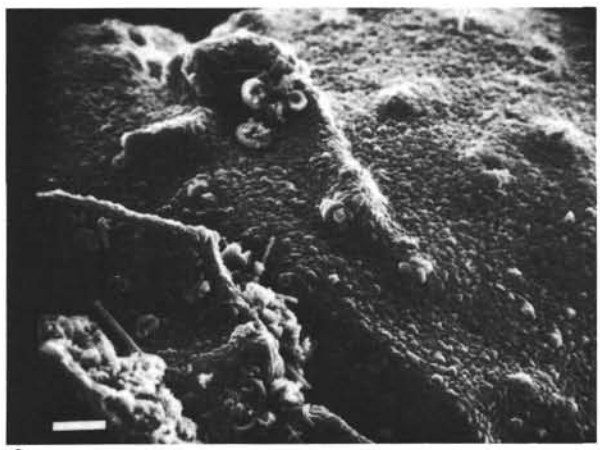
6

Plate 2. Site 577. **1.** *Aragonia* (Finlay), Sample 577-12-5, 80 cm. Bar = 100 μm. **2.** *Bulimina* (Cushman), Sample 577-12-5, 80 cm. Bar = 100 μm. **3, 4.** *Aragonia* (Finlay), Samples 577-12-5, 80 cm and 577-12-5, 128 cm. Bar = 100 μm. **5, 6.** Contrasting surface textures of two *Aragonia*, Sample 577-12-5, 128 cm. Bar = 10 μm.

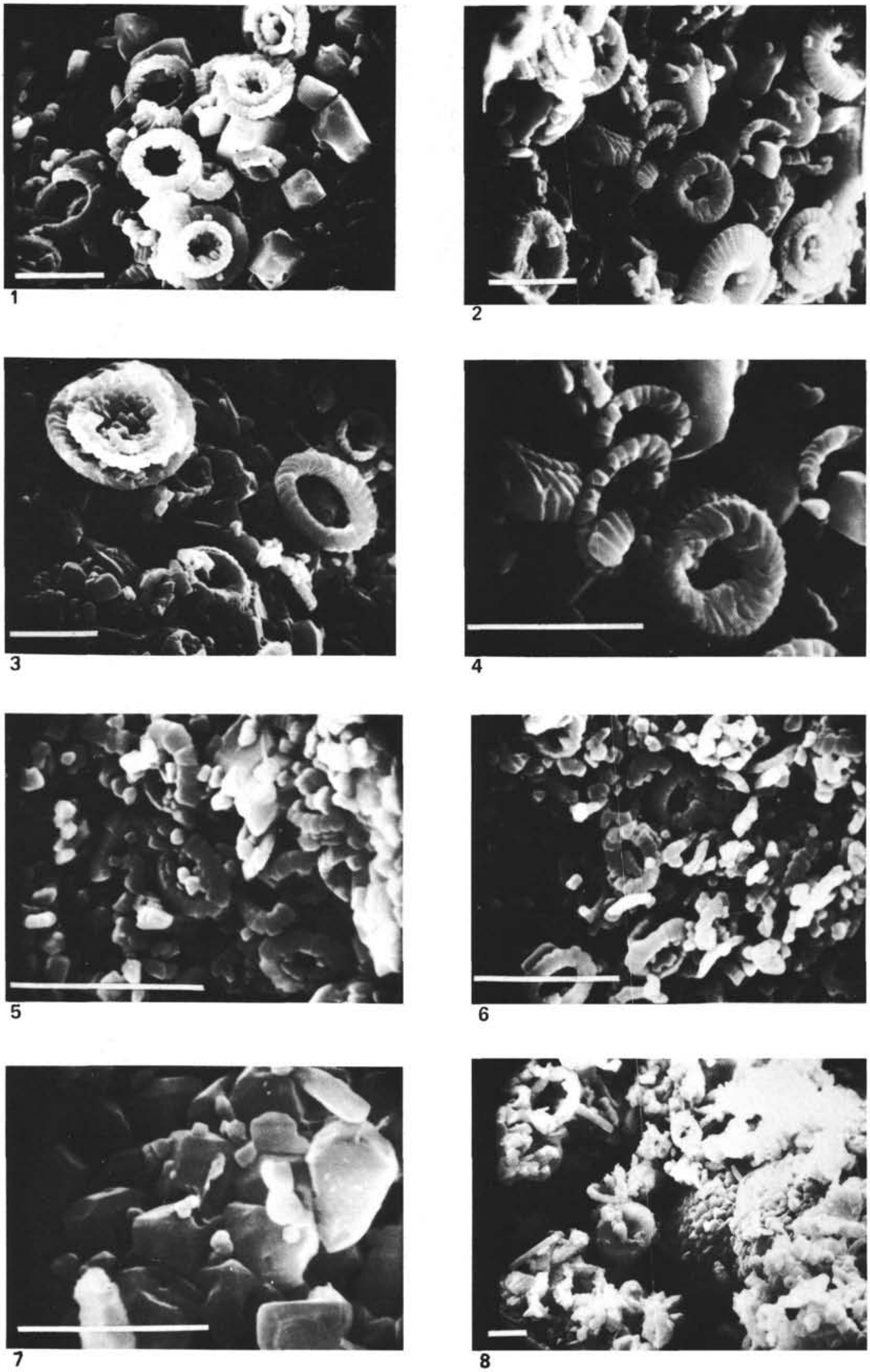

Plate 3. (Bar represents 10 μm.) **1–4.** Moderate to well preserved Danian calcareous nannofossil assemblage. Note the lack of overgrowths and etchings on the coccolith shields, Sample 577-12-2, 50 cm. **5, 6.** Coccoliths and coccolith fragments from Zone NP2. Calcite overgrowths are present on some specimens, Sample 577-12-5, 80 cm. **7.** Surface of a planktonic foraminifer from the boundary, sample 577-12-5, 125 cm. **8.** Coccolith ooze with foraminifer test in background, Sample 577-12-5, 125 cm.

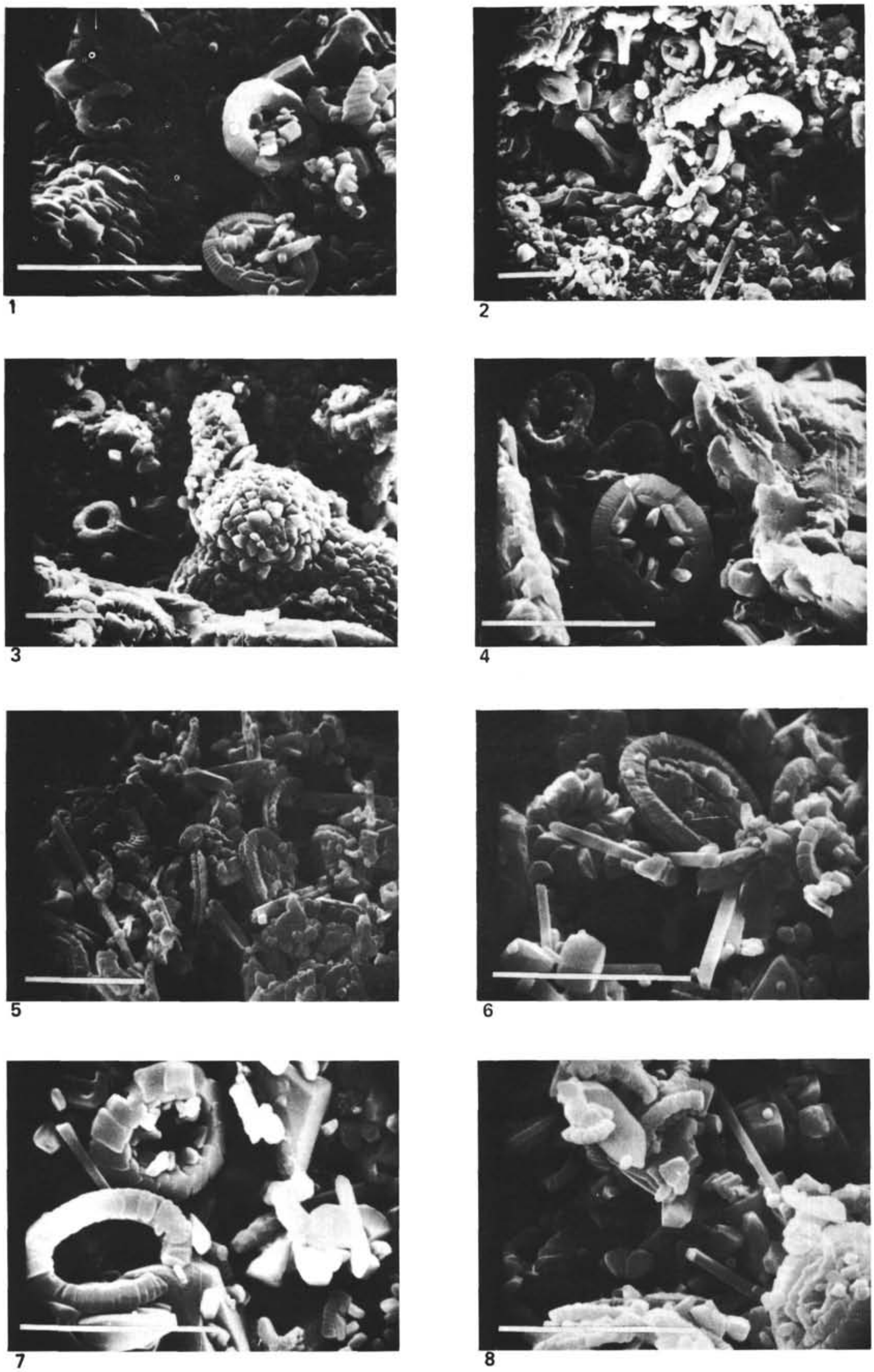

Plate 4. (Bar represents 10 μm.) **1–4.** Various calcareous nannofossils from boundary samples. Most specimens are moderately to well preserved. Overgrowths can be seen on several coccolith shields. Sample 577-12-5, 128 cm. **5–8.** Coccolith ooze of Maestrichtian age. Euhedral calcite overgrowths are present on most coccolith specimens. Partially disaggregated shields and fragments are also present.